Study on the Influence of Process Parameters of WEDM on the Machinability of D2 Steel

A Dissertation Submitted
In Partial Fulfillment of the Requirements
for the Degree of

Master of Engineering

in

Production Engineering

by

Amanpreet Singh
Registration No.: 801382002

Under the Supervision of
Dr. Hiralal Bhowmick

MECHANICAL ENGINEERING DEPARTMENT

THAPAR UNIVERSITY , PATIALA

July, 2015

CERTIFICATE

I hereby declare that the thesis entitled **"Study on the influence of process parameters of WEDM on the machinability of D2 steel"** is an authentic record of my work carried out as requirements for the award of the degree of **Master of Engineering** in **Production Engineering** at **Thapar University, Patiala** under the supervision of **Dr. Hiralal Bhowmick**, Assistant Professor, Mechanical Engineering Department, Thapar University, Patiala during July, 2013 to July, 2015. No part of matter embodied in this report has been submitted to any other university or institute for the award of any degree.

Date: 14/07/2015 ~~29/06/2015~~

Amanpreet Singh

It is certified that the above statement made by the student is correct to the best of my knowledge and belief.

14/7/15

Dr. Hiralal Bhowmick
Mechanical Engineering Department
Thapar University, Patiala – 147004

Countersigned by

Dr. S. K. Mohapatra
Sr. Professor & Head
Mechanical Engineering Department
Thapar University, Patiala – 147004

Dr. S. S. Bhatia
Dean of Academic Affairs
Thapar University, Patiala - 147004

Acknowledgement

I take the opportunity to express my heartfelt gratitude to my supervisor **Dr. Hiralal Bhowmick** for his unreserved guidance, constructive suggestion and for encouraging me at important junctures in the research work.

I would like to express my gratitude towards **Dr. Anirban Bhattacharya** and **Dr. Tarun Nanda** who took keen interest in my report and allowed me to access facilities of Mechanical Engineering Department laboratories. I am thankful to MED faculty for support and guidance. They gave me essential valuable advice, positive, criticism, thoughts and constant encouragement through discussions. I am thankful to Mr. Narinder Singh for assisting and guiding me in laboratory work.

I am grateful to **Mr. Rajinder Singh** (Proprietor), M/s Aman Metal Products, Ludhiana for allowing me with an opportunity to work on Wire Electrical Discharge Machine installed in his industry. This work and experience has not only enriched me with technical knowledge but has also imparted the maturity of thought and vision, the attributes required to be a successful mechanical professional. Sincere thanks to all my classmates for their support and assistance throughout the project.

I would also like to thank **Dr. S.K. Mohapatra, HOD, MECHANICAL DEPARTMENT** who motivated me to complete the report of my research work with enthusiasm and hard work.

I would like to express my heartfelt appreciation to my loving parents; I am unable to find words to embed my deep sense of gratitude for them.

Amanpreet Singh

AMANPREET SINGH

Abstract

Wire Electrical Discharge Machining process has significantly improved with the latest requirements in the industry. Wide capabilities of WEDM have allowed it to be used in production of aerospace and automotive industries. WEDM is a process in which a thin wire as electrode is used to transforms electrical energy to thermal energy which melts and removes the material. This process can be used to machine high strength alloy steels, conductive ceramics and aerospace materials.

The literature survey reveals that little research has been conducted on the comparison of wires to machine alloys having high hardness. Most of the research has been conducted with plain brass wire. It is well known fact that high material removal rate and high surface finish could not be obtained simultaneously. Brass wires produce high MRR but give poor surface finishing.

So, the purpose of this dissertation is to optimize the process parameters of WEDM using two different wires; plain brass and zinc coated brass, of same diameter and D2 steel (hardened) is used as workpiece material due to its high hardness and wide use in mechanical industry.

Pilot investigation is performed to find out significant factors and their levels by varying one factor at a time (OFAT approach). Taguchi's methodology is used to perform main investigation. S/N ratio and ANOVA techniques are used to examine results. L18 mixed OA is used with one factor at six levels and three factors at three levels. Peak current is varied at six levels. Factors for experiments are chosen by performing pilot study on maximum factors available and subsequently significant factors are considered. The four factors; Pulse on Time, Pulse off Time, Peak Current and Spark Gap Set Voltage are considered to examine their effect on performance characteristics that are material removal rate, kerf width and surface roughness.

The size of the specimen machined is *10 mm* 10mm* 10mm*. Two trials are taken for each experiment and total number of specimen machined is 72. The results were analyzed for single response optimization using Taguchi's delta statistic utility to find the optimum levels of four parameters for high material removal rate, low surface roughness and low kerf width. Multi response optimization is performed using multiple response signal noise (MRSN) technique. As per industrial machining requirement, both material removal rate and surface

roughness are equally important. In this technique, equal weightage is given to material removal rate and surface roughness, so that optimum levels of parameters can be obtained for high MRR and low surface roughness simultaneously.

The result data for material removal rate, kerf width and surface roughness obtained from the machining with both wires i.e. plain brass wire and zinc coated brass wire, is compared to examine parametric effect of both wires. The comparative study reveals that zinc coated wire is more superior in case of material removal rate and surface roughness as compared to plain brass wire.

The surface topography is examined on SEM to find out the thickness of recast layer obtained when machined with both wires and results are also compared for lesser recast layer. The SEM images and the EDX spectroscopy reveals the addition of different materials to the workpiece surface from wire surface during machining which in turn reveals the underlying mechanism of the formation of craters, debris and material deposited in the machined surface.

Key words: WEDM; AISI D2 steel; Zinc coated brass wire; Plain brass wire; SEM; EDS; Taguchi's L18 OA; ANOVA; MRSN.

Contents

List of Figures

List of Tables

Nomenclature

$\propto_{MRR}$ = Predicted value of material removal rate (Plain brass wire)

$\propto_{SR}$ = Predicted value of surface roughness (Plain brass wire)

$\propto_{Kerf}$ = Predicted value of kerf width (Plain brass wire)

α'_{SR} = Predicted value of surface roughness (Zinc coated brass wire)

α'_{MRR} = Predicted value material removal rate (Zinc coated brass wire)

α'_{kerf} = Predicted value of kerf width (Zinc coated brass wire)

μ_{MRR} = Overall mean for material removal rate with plain brass wire

μ_{SR} = Overall mean for surface roughness with plain brass wire

μ_{kerf} = Overall mean for kerf width with plain brass wire

μ'_{MRR} = Overall mean for material removal rate with zinc coated brass wire

μ'_{SR} = Overall mean for surface roughness with zinc coated brass wire

μ'_{kerf} = Overall mean for kerf width with zinc coated brass wire

µm = Micrometer

µs = Microsecond

Acronyms

ANOVA ≡ Analysis of variance

CNC ≡ Computerized Numerical Control

C_s ≡ Cutting speed

Cu ≡ Copper

DoE ≡ Design of Experiment

d_w ≡ Diameter of wire (mm)

EDM ≡ Electrical Discharge Machining

EDX ≡ Energy Dispersive X-Ray Spectroscopy

g ≡ Grams

HRC ≡ Rockwell Hardness Number in C scale

I_P ≡ Peak Current

k ≡ Kerf Width (mm)

l_g ≡ Length of spark gap

mm	≡	millimeter
MRR	≡	Material Removal Rate
MRSN	≡	Multiple Response Signal to Noise Ratio
OA	≡	Orthogonal Array
R_a	≡	Surface Roughness
SEM	≡	Scanning Electron Microscopy
S/N	≡	Signal to noise ratio
SR	≡	Surface Roughness
S_V	≡	Spark Gap set voltage
T_{OFF}	≡	Pulse Time Off duration
T_{ON}	≡	Pulse Time On duration
t_w	≡	Workpiece thickness
WEDM	≡	Wire Electrical Discharge Machining
W_F	≡	Wire Feed
W_T	≡	Wire Tension
Zn	≡	Zinc

Chapter 1

Introduction

1.1 Introduction

Electrical Discharge Machining is one of the earliest non-conventional manufacturing processes. EDM has been used to machine advanced materials with desired shape, size and required accuracy. In EDM process, electrically conductive materials are machined by using precisely controlled sparks that occur within the gap of an electrode and a work-piece in the presence of dielectric fluid. The two principal type of EDM processes are the die sinking and the Wire EDM process.

1.2 Mechanism of Wire EDM process

Wire EDM is an electrical discharge machining process with a continuously moving conductive wire as the tool electrode and material is eroded by successive electric sparks generated by current supply. Copper, brass, molybdenum etc. conducting materials are used in wire form as tool electrode. Generally de-ionized water is used as dielectric liquid in WEDM. The high heat generation results in melting and vaporizing of the tool and work piece. In EDM, the thermoelectric source of energy is used to erode material in a controlled manner through a series of electric sparks. Workpiece and the electrode are immersed in dielectric which is electrically non-conductive in nature. Dielectric used act as a coolant and also flushes away the debris. Heat generated at each electrical spark is around 8000 ^{0}C to 12000 ^{0}C. The WEDM is largely used in manufacturing dies and moulds. The WEDM's CNC system has the capability to control movement of wire and perform machining at high accuracy. The wire diameter ranges from 0.05 to 0.35 mm. The intricate shapes and smaller corner radii can be achievable with very thin wires. There is no mechanical stress induced during machining process as wire does not touch the workpiece. The WEDM is an exceptional machining process for manufacturing of tough material parts that are highly challenging to machine by traditional machining processes. Mostly, the wires are used only once for machining and discarded after use.

1.3 Wire-Cut EDM Machine

There are four basic elements of WEDM machine tool, the power supply system, the positioning system, the drive system and the dielectric system. All the four basic sub systems are distinct from conventional EDM.

1.3.1 Power Supply System

WEDM power supply system comprises of electric pulse generator, motor driver units for positioning system and CNC controller. It differs from conventional EDM power supply system basically in pulse frequency which is about 1 MHz that results in reduced crater size and better surface finish. Such high frequency ensures that each spark removes as little material as possible, thus reducing the size of crater. The diameter of wire in WEDM is small that limits its current carrying capacity to a small value. Power supply converts alternating current (AC) into direct current (DC) to generate sparks in the machining zone. It can also regulate various process variables like voltage, current, pulse on and off duration, duty cycle and electrode polarity.

1.3.2 Positioning System

The WEDM machine constitutes of a primary table (X-Y), a secondary table (U-V) and mechanism for wire drive. Workpiece is clamped on primary table. Primary table has the capability to move along X-axis and Y-axis which is controlled with servo motors. Secondary table plays the role to control movement of wire guides which are installed on opposite sides through which the wire moves under tension through the workpiece. The wire travelled continuously through workpiece from wire feed pool and round up on spool. The wire guide below table height is stationary where as the upper wire spool guide is supported by the U-V table. The upper wire guide can also be positioned vertically along Z-axis. Figure 1.1 shows the various functional parts of WEDM process.

As the operation advances, the X-Y controller change the position of worktable which carries the work piece in transverse direction along a proposed track programmed in the CNC controller. Dielectric fluid also works as a flushing agent, as the machining operation is continuous, there is a need to remove away the debris from machining zone. The nozzles present on both sides of workpiece supplies the water to flush the debris away from gap. Ionised water is used as a dielectric medium in WEDM, kerosene oil is used in RAM EDM

and no fluid is used in dry EDM; Ion exchanger resin is used to prevent the ionisation of water.

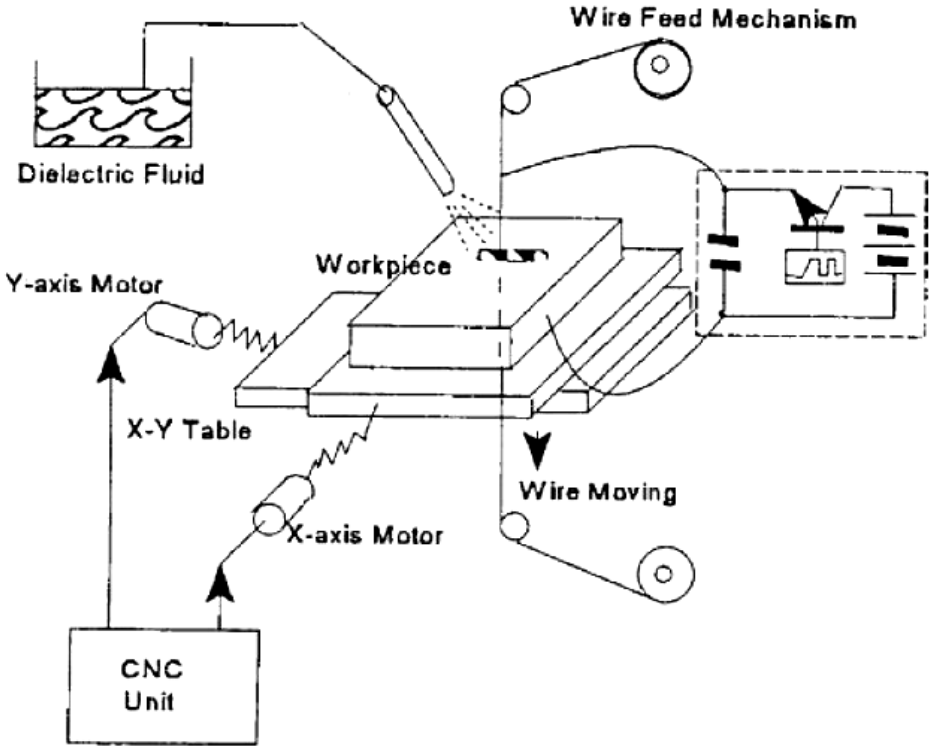

Figure 1.1: WEDM Process [Saha et al., 2004]

1.3.3 Wire Drive System

The wire travelled continuously through workpiece from wire feed pool and round up on spool in waste box. The wire guide below table height is stationary where as the upper wire spool guide is supported by the U-V table. The wire is fed under tension to decrease mechanical vibrations during discharge explosion. The upper wire guide can be displaced transversally, along U-V axes, with respect to the lower wire guide, whereas lower wire guide is stationary. This system serves two purposes continuously delivers fresh wire, and always keeps the wire under tension so that it moves in the machining zone as a straight wire. The latter requirement is for the nature of machined surface. It also minimizes the "wire-breaks" during machining. As it moves towards take up spool, the wire passes through series of tensioning rollers.

1.3.4 Dielectric System

The dielectric system consists of dielectric fluid, reservoir, filters, pump and delivery devices. During machining, the nozzles provide the pressurized water to take away debris from machining zone. The main purpose of dielectric is to provide non conducting atmosphere around the wire and workpiece to avoid premature discharge. Dielectric also works as a coolant for machining zone.

1.4 Process Parameters

In WEDM, there are many process variables which influence the response machining characteristics. Machining conditions can be controlled through controlling these process parameters. Optimum levels of process parameters play a very significant role in manufacturing process. To achieve high MRR or low surface roughness, proper selection of process variables is necessary. In WEDM, each parameter has a range in which it can be changed for required machining condition. Various process variables in WEDM are:

- Pulse On Time (T_{on})
- Pulse Off Time (T_{off})
- Peak Current (I_P)
- Spark Gap Set Voltage (S_v)
- Wire Feed (W_F)
- Wire Tension (W_T)
- Peak Voltage
- Flushing Pressure (W_p)

1.4.1 Pulse On Time (T_{on})

Pulse on time in microseconds describes the period in which current flows in WEDM. During this period of time, spark generates heat between the electrodes which results to rise in temperature which is directly proportional to current applied. High duration of pulse on time leads to high cutting rate. In this machine tool, the T_{ON} can be varied in the range of 0.1 µs to 1.65 µs. High T_{ON} duration can cause wire breakage and also leads to high surface roughness.

1.4.2 Pulse Off Time (T_{off})

It is the time between two simultaneous sparks. There is no supply of current in this interval. The T_{off} represents the period of time in microseconds (μs). As the T_{off} period decreases, number of discharges increases in a specified period which results in rise in spark efficiency. The purpose of providing pulse off time is to decrease wire breakage which may reduce cutting efficiency. It also enhances the stable machining environment.

1.4.3 Peak Current (I_P)

The peak current in WEDM is the maximum current passing through the wire and workpiece. Discharge energy directly depends upon the peak current. High value of peak current results in high cutting rate

1.4.4 Spark Gap Set Voltage (S_v)

It is the voltage which represents the actual gap between electrodes. The available range of S_v in WEDM is 00-99 which is applied in steps of 1 unit (Volt). Figure 1.2 shows the S_V setting for two different gaps viz. 80 V and 30 V.

The smaller the gap voltage:

- The faster it cut
- The smaller the distance between wire and workpiece, lesser will be the area for the chips to flush out of the wire/workpiece gap.
- The chances of breaking of wire increases.

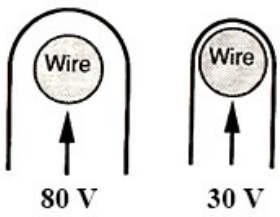

Figure 1.2: Spark Gap Set Voltage [W.1]

1.4.5 Wire Feed (W_F)

In WEDM, wire travels through the wire guides and rate at which wire travels can be defined as wire feed. It is fed continuously for sparking through the wire guides to the workpiece. It is always desirable to set the wire feed to maximum. If the wire feed is set at maximum value, it

will result in less wire breakage. This also leads to better machining stability. The W_F setting range available on the machine tool is 01-15 unit which is applied in steps of 1 unit.

1.4.6 Wire Tension (W_T)

Wire tension describes the load applied between the upper and lower wire guides. It stretches the wire and keeps it straight to diminish vibrations of wire during machining. It is a gram equivalent load. More the thickness of job more is the tension required. Proper setting of wire tension is must to ensure accurate cutting and to avoid wire breakage. The W_T setting ranges from 01-15 units which is applied in steps of 1 unit.

1.4.7 Pulse Peak Voltage

Pulse peak voltage setting is for selection of open gap voltage. Discharge energy increases with increase in pulse peak voltage results in high cutting rate.

Figure 1.3 shows the formation of big size craters when higher settings of pulse peak voltage is used and results into rapid cutting rates, high surface roughness and larger chips formation.

Figure 1.3: Rough Surface Finish [W.1]

Figure 1.4 shows the formation of small size craters when lower settings of pulse peak voltage is used and results into slow cutting rate, better surface finish and smaller chips formation.

Figure 1.4: Smooth Surface Finish [W.1]

It is useful to process manufacturing at low spark energy setting with high frequency of sparks and chip size will get reduced. The rapid cutting operation can be achieved with better flushing of chips. Figure 1.5 shows the variation produced in chip size with change in spark energy.

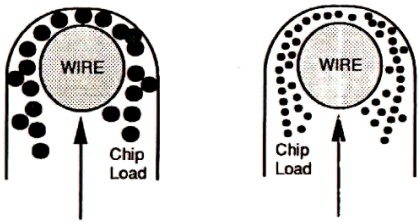

Figure 1.5: Variation in Chip size with spark energy [W.1]

1.4.8 Flushing Pressure (W_p)

It can be defined as the pressure with which the dielectric fluid is supplied to the electrode-workpiece interface. The flushing pressure range on WEDM machine is either 1 (High) or 0 (low). The requirement for high flushing pressure is when workpiece to be cut is of high thickness or when discharge energy is high. Trim cuts and thin workpiece require low pressure mode. Flushing pressure also results in removal of debris from the interface.

1.5 Performance Parameters

The performance parameters can be described as the response machining characteristics or output machining performance of WEDM process. The input process variables are varied to get the desired results for machining. These results are in the form of performance parameters. They are the results of the machining by which the quality of machining process can be evaluated. Various performance parameters in WEDM are:

- Material Removal Rate (mm^3/min) or Cutting Rate (mm/min)
- Surface Roughness (μm)
- Kerf Width (mm)
- Dimensional Deviation (mm)

1.5.1 Cutting Rate or Material Removal Rate

Cutting rate can be defined as the cutting speed of WEDM i.e. distance travelled during machining per unit time. It is measured in mm/min. It should be high to increase productivity. High cutting speed leads to shorter machining cycle time. In WEDM process, cutting speed is displayed on the screen of machine. Eq. (1.1) defines material removal rate as total material removed during machining by the electrode and it is measured in mm^3/min.

$$MRR = C_s \times t_w \times k \quad (1.1)$$

Where;

MRR= Material Removal Rate

C_s =Cutting Speed

t_w =Thickness of workpiece

k =Kerf Width

1.5.2 Kerf Width

The kerf width is the width of cut produced during machining when the wire passes through workpiece. It is measured with the help of a Nikon Profile Projector V-10A. As defined in Eq. (1.2), kerf width is sum of diameter of wire and twice the gap between wire surface and workpiece. Figure 1.6 shows the schematic view of width of cut.

$$k = d_w + 2(l_g) \tag{1.2}$$

where;

k =Kerf Width

d_w = Diameter of wire

l_g =length of spark gap

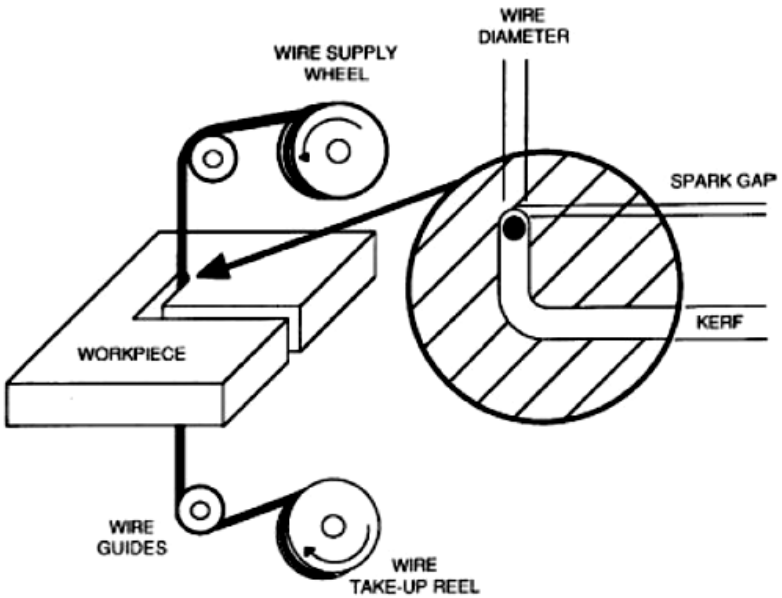

Figure 1.6: Schematic view of Kerf Width [Tosun et al., 2004]

1.5.3 Surface Roughness

The surface roughness is due to a series of regularly repeated deviations of a wave, these deviations are produced by the trace of an edged cutting tool and plastic flow of metal while machining or erosion of metal by vaporization due to high temperature machining like in EDM. The average roughness (R_a) is generally used to measure surface roughness. R_a is measured by comparing all the peaks and valleys to the mean line, and then taking mean of all for the defined cut-off length (generally it is taken as 0.08 mm) and rated in micron (μ). Cutoff length can be defined as range in which stylus moves over the surface. For better and accurate result, longer cutoff length is required.

1.6 Advantages of WEDM Process

WEDM has more efficient machining potential than other non conventional cutting processes.

- There is no contact between electrode and workpiece, so it eliminates the mechanical stress induced during machining.
- Wire EDM process has the capability to machine materials that have tremendous strength and are high temperature resistive.
- It eliminates the occurrence of geometrical changes in the machining of hardened steels.
- Intricate parts and fragile shapes, including micro geometries or intricate shapes, contours, cavities can be machined easily by WEDM process.
- The tolerances of +/- .0025 mm can be achieved by this process.
- Machine can run unattended over night for machining workpiece.

1.7 Disadvantages of WEDM Process

- It is expensive to install this machining process.
- The formation of recast layer is one of the problems in this process.
- Some of WEDM process like trim cut or high surface finish cut runs at slow cutting rate which increases the productivity cost.
- There is a limit to the type of workpiece to be machined by this process. It can be a height issue or non conductivity of material. Large parts can’t be machined at every WEDM.

1.8 Applications of WEDM Process

WEDM was basically developed for the tool and die industry. The growth in machining rate, safety, unattended operations and accuracy has grown it into many industries. These days, WEDM has great demand in medical, aerospace, automotive, defence, electronics and extrusion applications.

It is suitable to machine thick sections of material. It can machine material having thickness up to 220 mm. The CNC part of WEDM proves to be very useful as it can machine the parts with full accuracy and is very useful in the manufacturing of die of different types at large scale. The fabrication process that needs hours to manufacture tools for conventional EDM that needs some other finishing processes like polishing and grinding to prepare tools and machining time can be shortened by using WEDM. The WEDM can reduce the processing time by 35%

Chapter 2

Literature Review

2.1 Literature Review

Liao and Huang [2003] conducted experiments on WEDM on SKD11 alloy steel and brass wire using Taguchi's L18 mixed OA technique. The input parameters viz., wire feed rate, pulse on time (T_{on}), pulse off time (T_{off}), wire tension (W_T), wire velocity and fluid pressure were studied to measure response parameters viz., material removal rate, gap width and surface roughness (R_a). According to S/N ratio and ANOVA analysis, it was found that wire feed rate and T_{on} have influenced more in case of MRR and T_{on} was the sole significant parameter for R_a.

Tosun et al. [2004] studied experiments on AISI 4140 steel on WEDM with brass wire used as electrode. They examined various process parameters to study effects on material removal rate and kerf width. Taguchi's L18 mixed OA was used, with open circuit voltage varying at two levels and rest at three levels. Analysis of results was performed with S/N ratio and ANOVA technique. Open circuit voltage (63.44%) and pulse duration (28.7%) were found significant in kerf width. Open circuit voltage (78.67%) and pulse duration (12.76%) were found significant in case of MRR. Confirmation Experiments were conducted for the predicted optimum process parameters and were found close to predicted values.

Hascalyk and Caydas [2004] investigated the surface topography and surface metallurgy of D5 tool steel workpiece machined on WEDM with brass wire used as electrode. Based on the micro-hardness and micrographs of their results, they identified the four zones formed after machining. Zones were recast layer, white layer, annealed area and parent material. It was found that thickness of white layer as well as cracks in white layer increased with increase in open circuit voltage and pulse on time.

Ramakrishnan and Karunamoorthy [2006] conducted experiments on heat treated D2 steel material with zinc coated brass wire used on WEDM. Taguchi's L16 OA was used to perform experiments with five input parameters, viz., T_{ON}, W_T, delay time, W_S and I_P. In this study, MRR, surface roughness (SR) and wire wear ratio (WWR) were selected as machining parameters. The experimental data were analyzed by MRSN and ANOVA and their results showed that pulse on time (T_{ON}) and ignition current intensity ($I_{P)}$ were the significant

parameters. The confirmation experiment showed that MRR was raised by 1.5 times, SR decreased by 1.2 times and WWR was decreased by 1.2 times.

Mahapatra and Patnaik [2006a] performed experiments on Robofil CNC WEDM using Zn coated copper wire as electrode and D2 steel as work-piece material. L27 OA was used to find out optimum parametric levels for high MRR and less surface finish. The input parameters selected were discharge current, pulse duration, pulse frequency, wire speed, wire tension and dielectric flow rate and two interactions were considered. The S/N ratio for both machining parameters were calculated and it was found that discharge current, pulse duration, dielectric flow rate and both interactions have significant effect and rest single factors have less significant effect on MRR as well as on surface finish. Analysis of the results had suggested optimum levels of selected factors for maximization of MRR and SF.

Mahapatra and Patnaik [2006b] performed an experimental study on robofil WEDM using zinc coated copper wire and D2 alloy steel as workpiece. Experiments were operated using Taguchi's L16 OA. Six control factors selected were discharge current, pulse duration, pulse frequency, wire speed, wire tension and dielectric flow rate. they selected five interaction. The machining performance was calculated by using S/N ratio analysis for higher the best (MRR) and lower the best (SR). It was found that factor discharge current, pulse duration, pulse frequency along with their interactions were significant for MRR and SF. Confirmation experiment was performed to validate the conclusion drawn during analysis phase and was found that it agree well with predicted optimal setting with an error of 4.94% for MRR and 1.059% for SR.

Mahapatra and Patnaik [2007] conducted experiments to examine the influence of process variables on machining characteristics on WEDM using zinc coated copper wire and D2 steel as workpiece material. The response parameters selected were material removal rate, surface finish and kerf. Six parameters viz., discharge current, pulse duration, pulse frequency, wire speed, wire tension and dielectric flow rate and two interaction of discharge current with pulse duration and dielectric flow were selected, while Taguchi's L27 OA was used and experimental observation were transformed into S/N ratio. The better machining performance was represented by 'higher is better' for MRR and 'lower is better' for both surface roughness as well as kerf. It was found factor discharge current, pulse duration and interactions were significant for MRR and SF. In case of kerf, wire speed was most significant among all factors and dielectric flow rate was least significant.

Shah et al. [2009] conducted experiments on tungsten carbide with brass wire used as electrode on WEDM. In this study, eight process parameters were selected to examine their influence on machining performances; material removal rate, kerf and surface roughness. Taguchi's L27 OA was selected for experiments with three levels each. S/N ratio and ANOVA techniques were applied to examine the results. Material thickness was considered as a factor with three varied thicknesses. The pulse on time, pulse off time, open voltage and servo voltage were significant factors, whereas material thickness didn't affect the MRR and kerf width. Wire tension plays important role as far as kerf width was concerned and was not significant in MRR and surface roughness. Material thickness was significant in results of surface roughness; larger material thickness gave the better surface finish. It was also found that kerf width widens with rise in pulse on time and increasing wire tension decreases it.

Singh and Garg [2009] considered six input parameters to examine material removal rate of H-11 steel on WEDM with brass wire as electrode. Experiments were taken by varying one input parameter and other parameters were fixed at some mean fixed value. Results showed that MRR increases with increase in pulse time on and peak current. MRR decreases with increasing pulse off time and spark gap voltage. Wire tension and wire feed has no effect on MRR as it remains constant on varying both parameters.

Kumar et al. [2010] worked on incoloy800 super alloy to optimize multi quality characteristics for MRR, surface roughness and kerf. Taguchi's L9 OA array was applied to execute experimentation by varying levels of four factors and optimization has been done using grey relational analysis. ANOVA was used to analyze results and to find percentage contribution of each factor. Confirmation experiments showed the improvement of 7.74% in MRR, 6.34% in surface roughness and 8.64% in kerf width.

Jangra et al. [2010] performed WEDM experiments on D3 die steel. Taguchi's L18 mixed OA used by varying peak current at six levels and pulse on time, pulse off time, wire speed and wire tension at three levels each. The selected machining performance measures were cutting speed (mm/s), surface roughness and dimensional lag. Significance of factors was measured using ANOVA for grey relational grade. Grey relational technique was used for multiple optimum process parameters for maximum cutting speed and minimum surface roughness and dimensional lag. Confirmation experiments showed the acceptable results with respect to predicted values of three performance parameters.

Khanna and Singh [2011] conducted experiment on cryo-treated D3 workpiece in WEDM. The number of input parameters were six each varied at three levels to cutting rate. L27 OA

was used to design experiments. ANOVA of mean data and S/N data was calculated to find significant factors. They observed that the cutting rate tend to decrease with increase in pulse width, time between two pulses and spark gap voltage. The values obtained from confirmatory experiments at optimum levels of parameters for high cutting rate were found within predicted confidence intervals.

Soo et al. [2011] presented experimental data for workpiece machining on WEDM for $Ti_6Al_2Sn_4Zr_6Mo$ titanium alloy. Copper core coated wires were used. It had been observed that 70% improvement in production was possible as compared to plain brass wires with the similar operating conditions. They concluded that this could be furthered raised by increasing pulse on time. The different sections on the specimen surface had different surface roughness due to irregular sparks generated. The erosion of wire tool lead to wider machining gaps.

Kumar et al. [2012] conducted experiments on WEDM on pure titanium (grade-2) material with aim to model the surface roughness with RSM technique. The response of input parameters was measured using multi-response optimization approach to optimize the surface roughness. ANOVA was applied to find significant parameters and pulse on time, pulse off time, peak current and spark gap voltage were found to be significant. The wire feed and wire tension found to be insignificant to the output process parameters.

Goyal et al. [2013] investigated the effect of two different cryogenic treated wires on D3 steel material with WEDM process. Performance measuring characteristics chosen was material removal rate (g/min). Taguchi's L9 OA was opted for experimentation design and results were analyzed by S/N ratio technique. It was found that cryo treated zinc brass wire perform better than plain brass wire for material removal rate. The various input parameters selected were pulse width, time between two pulses, wire tension and wire feed rate. Wire tension and wire feed effects were constant and pulse width was found most significant. It was found that zinc coated brass wire was 22.55% more efficient than plain brass wire in term of material removal rate.

Dhobe et al. [2013] conducted experiments on WEDM using brass wire as electrode. D2 steel heat treated in two different ways was used as workpiece. The first one was Single Tempered (ST) after hardening and other was Double Tempered (DT) after hardening. The input parameters were pulse on time (T_{on}), pulse off time (T_{off}), servo voltage(S_v) and peak current(I_p) and in their analysis, one factor at a time were considered and all other parameters were set to be constant to find out effects on output parameter i.e. surface roughness(R_a).

Surface roughness increased with increase in T_{on} and I_p, decreased with increase in T_{off} and S_v. It was found that DT after hardening reduces surface roughness compared to ST.

Mann and Chaudhary [2013] investigated the effects of four controllable variables of WEDM viz., pulse on time(T_{on}), pulse off time(T_{off}), servo voltage(S_v) and peak current(I_p) on the material removal rate(MRR) and surface roughness(R_a). The workpiece material used was D2 steel and electrode was brass wire. RSM and ANOVA methodology was used to analyze performance parameters. It was found that $T_{on,}$ $T_{off,}$ and S_v have maximum influence on MRR, T_{on} and T_{off} have significant effect on R_a and I_p in MRR, S_v in R_a are very less influencing.

Ikram et al. [2013] conducted experiments on D2 steel using brass wire for optimization of eight control factors viz., material thickness, pulse on time(T_{on}), pulse off time(T_{off}), servo voltage(S_v), wire speed, dielectric pressure, open voltage and wire tension(WT). The response characteristics were on material removal rate (MRR), surface roughness (R_a) and kerf. Taguchi L18 mixed OA was applied for experimental design. ANOVA and S/N ratio were used to identify the significant process parameters and to achieve optimum levels. From their study it was found that for R_a, significant parameters are T_{on} and open voltage and for kerf T_{on}, W_T and for MRR significant factors are T_{on} and $S_{v.}$ Material thickness didn't have significant effect in either case. They recommended that pulse on time and open voltage should be kept at lowest level for getting minimum surface roughness and it was opposite in case of MRR.

Sharma et al. [2013] optimized the WEDM process parameters for multiple response characteristics using RSM technique on HSLA 100 workpiece with brass wire. The central composite rotatable design (CCRD) has been applied to design experiments. ANOVA was used to check significance factors for MRR and surface roughness. They studied the individual effect of different parameters and their interaction for high MRR and low surface roughness. Three experiments were performed for multi objective optimization. It has been observed that the calculated error for predicted value and confirmative experiments is small and lies within -5.18% to 5.65% for MRR and -3.35% to 4.19% for SR.and kerf at optimum levels of parameters.

Goyat et al. [2013] presented experimental data for cutting rate as machining characteristic in WEDM. D2 steel was used as workpiece and RSM technique has been used to design experiments. Experiments were performed according to Central Composite Rotatable design and ANOVA was done for result data. The results showed that almost every factor and their

interactions were found significant. The R-squared values found to be very accurate with value of .9997.

Sudharsun et al. [2013] conducted experiments on stainless steel on WEDM using brass wire as tool electrode. Taguchi's L16 OA was used to design experiments. Four factors were selected and varied at four levels. Taguchi's optimization technique was applied to find S/N values and main effect diagrams were plotted to illustrate behaviour of parameters at different levels of factors. Multi objective grey relational analysis has been used to find optimum levels for low surface roughness and low kerf width. ANOVA for grey relational grade showed that pulse on time is the significant factor for multi objective optimization.

Dhobe et al. [2014] performed experiments on cryo-treated AISI D2 tool steel on WEDM. Taguchi L9 OA was selected to design and conduct experiments by varying performance parameters viz., pulse on time(T_{on}), pulse off time(T_{off}), servo voltage(S_v) and peak current(I_p). Based on ANOVA and S/N calculation for machining parameter i.e. surface roughness, T_{on} was found to be the most significant factor (77.78%), I_p and S_v were significant (11.70% & 9.18%) and T_{off} (1.32%) was least significant.

Patil and Waghmare [2014] conducted experiments on Sodick WEDM to examine the conditions for maximum material removal rate (MRR). The response surface methodology (RSM) approach was used to perform experiments. The material selected was D2 steel and electrode used was brass wire. RSM approach was applied on three factors viz., pulse time on, peak current and wire tension each at three levels. It was observed that peak current was more significant than pulse on time and wire tension were less significant for material removal rate.

Bhatia et al. [2014] studied the effect of four process parameters on surface roughness on WEDM. D2 steel workpiece was selected with brass wire as electrode. Taguchi's L9 OA was applied to form experimentation design. The process variables were peak current, pulse on time, pulse off time and wire tension, each at three levels. S/N ratio and ANOVA techniques were used to analyze the data for surface roughness. The results showed that pulse off time has greater contribution in attaining less surface roughness. Optimum parameters were selected from S/N ratio values for lesser surface roughness. Predicted value was calculated for selected parameters and confirmation experiments showed error of 3.93%.

Shivdev and Shinde [2014] conducted experiments on D3 tool steel on WEDM with molybdenum wire as electrode. Pulse on time, pulse off time, peak current and wire tension were varied to examine their effect on material removal rate (mm^2/min), gap current and

dimensional deviation. Taguchi's L9 OA was used for experiments and results were analysed by S/N ratio technique to find optimum process parameters. Grey Relational Analysis was used for multi-objective characteristics optimization. The results showed that dimensional deviation for "smaller is better" approach, first increases than decreases with increase in process parameters. Peak current shows a significant effect on gap current whereas time on and time show less significant effect and the effect wire speed was constant on gap current.

Abhinesh et al. [2014] conducted experiments on two different titanium alloys (grade 5 & grade 2) with two different wires (brass wire and brass coated nickel wire) on WEDM. Taguchi's L16 OA was used having 5 process parameters; pulse on time, pulse off time, peak current, including material of wire and workpiece each having two levels. It was found that by taking first three factors at higher level, and using grade-5 and brass wire, higher material removal rate and lower electrode wear rate can be achieved.

Khundrakpam et al. [2014] studied the effects of five parameters on surface roughness of EN-8 steel with WEDM process. Taguchi's L27 OA (3*5) was used in which three interaction were considered between different factors. S/N ratio and ANOVA techniques used to find out optimal parameters for less surface roughness. Three parameters; Pulse time on, peak current and wire feed were significant and two interactions between pulse time on and peak current, peak current and wire feed were significant in results. Optimum levels of different factors were selected from S/N ratio table and predicted value was calculated for minimum surface roughness and confirmation experiment showed 5.39% error.

Chabra et al. [2014] investigated the effects of various process variables on material removal rate with WEDM process on P-21 die steel and zinc coated copper wire was used as electrode. Peak current was varied at six levels and rest factors at three levels, so Taguchi's L18 mixed OA was used for experimentations with factors and results were analyzed by S/N ratio technique. Most significant factor found was pulse off time and pulse on time. Material removal rate was majorly effected be these two factors and others were less significant.

Vates et al. [2014] investigated influence of six WEDM process parameters on D2 steel to evaluate surface roughness and material removal rate and chromium coated copper wire was used as tool electrode. RSM and ANN techniques were used to model experimentation and ANOVA was used to observe contributing factors. They have found that ANN proved to be best fitted model for surface roughness and RSM for MRR.

Tilekar et al. [2014] studied the effect of surface roughness and cutting width on aluminium and mild steel in WEDM and brass wire was used as tool electrode. Taguchi's L9 OA was

used to conduct experiments. Results were analysed using ANOVA to find significant factors for surface roughness and kerf width. The surface roughness was measured in longitudinal and transverse direction. The results for aluminium workpiece showed that T_{ON} was significant factor for surface roughness in longitudinal direction with contribution of 98% and in transverse direction T_{OFF} contributes up to 83%. In case of mild steel, I_P was the most significant factors in both longitudinal as well as transverse directions for surface roughness. The ANOVA results for kerf width showed that Wire feed was most significant factor for aluminium material and T_{ON} was most significant for mild steel. Confirmatory experiments for single objective optimization were performed to find low surface roughness.

2.2 Gap in the Literature and Selection of the problem

In the most of the past works only one output was studied and very few have studied 2 or more response parameters simultaneously. It is well established fact that a high material removal rate and a very good surface finish can't be achieved simultaneously in Wire- EDM. Till date, very few researchers have used zinc coated brass wire and studied comparison between the zinc coated brass and plain brass wire in the research. In majority of the past research work, plain brass wire is used for cutting purpose and very few used stratified wires such as zinc coated brass or zinc coated copper. Also, it may be noted that most of the prevailing approaches use complex mathematical models for optimization of multiple response. There also exist some other approaches like RSM, Grey relational Analysis which may be quite efficient for multi-response optimization of WEDM processes. Only few of them used relatively simpler computational procedures.

In past research, researchers have used soft D2 steel used as workpiece material and very few used hardened D2 steel and most work is done on D2 steel with EDM process and less work is performed on hardened D2 steel with Wire-EDM process.

Keeping this consideration in view, the present work describes the optimization of multiple performance characteristics. Taguchi method is used to achieve better material removal rate (MRR), surface finish (SR) and width of cut (kerf).

2.2.1 Statement of the problem

The present work "Study on the influence of process parameters of WEDM on the machinability of D2 steel" has been undertaken keeping into consideration the following facts:

- The past study on WEDM has revealed that the main parameters selected for the research were pulse on time, pulse off time, servo voltage, peak current, wire tension and wire feed. So, pilot study is conducted to study performance on machining characteristics by varying one at a time approach and to find significant parameters.
- Different wires with varying properties; some provide high MRR and some higher surface finish and materials with high strengths and capabilities are being developed continuously.
- The investigation of optimal machining parameters for this material is thus very essential with different wires.
- The predicted optimal solutions need to be verified experimentally using suggested combination of machining parameters.

2.2.2 Objectives

To determine the working ranges and levels of the WEDM process variables for the material and wires selected.

- Experimental investigation of the influence of various process parameters viz., pulse on time, pulse off time, spark gap set voltage, peak current, wire tension and wire feed, on the performance characteristics such as material removal rate (MRR), surface finish (SF) and kerf width.
- Single objective Optimization of the performance measures using Taguchi method for the D2 steel (hardened) which is mostly used in tool and die manufacturing industries.
- Multi objective optimization using multiple response signal noise (MRSN) technique to get optimum levels for high MRR and low surface roughness simultaneously.
- Comparison of MRR, surface roughness and kerf width at different levels of different parameters with two different wires viz., plain brass wire and zinc coated brass wire.
- To examine surface characteristics after machining and comparing the results obtained by machining with both wires.
- Verification of results by performing confirmative experiments and calculates the error or any improvement obtained by optimum levels of parameters studied in this research.

Chapter 3

Methodology and Design of Experiments

3.1 Machine Tool

The experiments were carried out on a Wire EDM machine (ELEKTRA SPRINTCUT 734) of Electronica Machine Tools Ltd. installed at Aman Metal Products, Focal Point, Ludhiana, India. Figure 3.1 shows the WEDM machine tool which has the following specifications:

Design:	Fixed column, moving table
Table size:	440 x 650 mm
Max. Workpiece height:	200 mm
Max. Workpiece weight:	500 kg
Main table traverse (X, Y):	300, 400 mm
Auxiliary table traverse (u, v):	80, 80 mm
Wire electrode diameter:	0.25 mm (Standard)
Generator:	ELPULS-40 A DLX
Controlled axes:	X Y, U, V simultaneous / independent
Interpolation:	Linear & Circular
Least input increment:	0.0001 mm
Least command input (X, Y, u, v):	0.0005 mm
Input Power supply:	3 phase, AC 415 V, 50 Hz
Connected load:	10 KVA
Average power consumption:	6 to 7 KVA

Figure 3.1: WEDM Machine Tool [Photo Courtsey: Aman Metal Products, Ludhiana]

3.2 Workpiece and Wire Materials

The hardened AISI D2 alloy steel plate of 130 mm × 133 mm × 10 mm size as shown in Fig. 3.2 has been used as work piece for investigation. The workpiece was procured from Sehgal Steel Traders, Focal Point, Ludhiana and hardening of material was processed at Central Tool Room, Focal Point, Ludhiana. It is a high carbon high chromium alloy tool steel. It shows high dimensional stability in heat treatment. D2 steel has high wear resistance. It has hardness in the range of 56-62 HR. It acquires mild corrosion resisting properties because of high content of chromium. Its chemical composition properties are obtained by performing spectroscopy and described in Table 3.1. Table 3.2 illustrates the physical properties of D2 steel. It has various applications as manufacturing of stamping or forming dies, punches, forming rolls, knives, slitters, shear blades and tools. Steel Blank is undergone the vacuum heat treatment process for enhancement of material properties such as hardness. At this process with 6 bar nitrogen gas quenching a cooling speed from austenitising temperature 980^0C to 520^0C of 28^0C/min in the surface was achieved to obtain a hardness of 62 HRC.

Table 3.1: Chemical Composition of material

Constituent	C	Si	Mn	P	S	Cr	Mo	V
% Composition	1.52	.37	.40	.04	.062	12.0	.56	.18

Table 3.2 Material Properties of D2 Steel [W.2]

Melting Point	1421 ℃
Density	7.7×10^3 kg/m^3
Thermal Conductivity	20 w/(m*k)
Vickers scale Hardness	748HV1

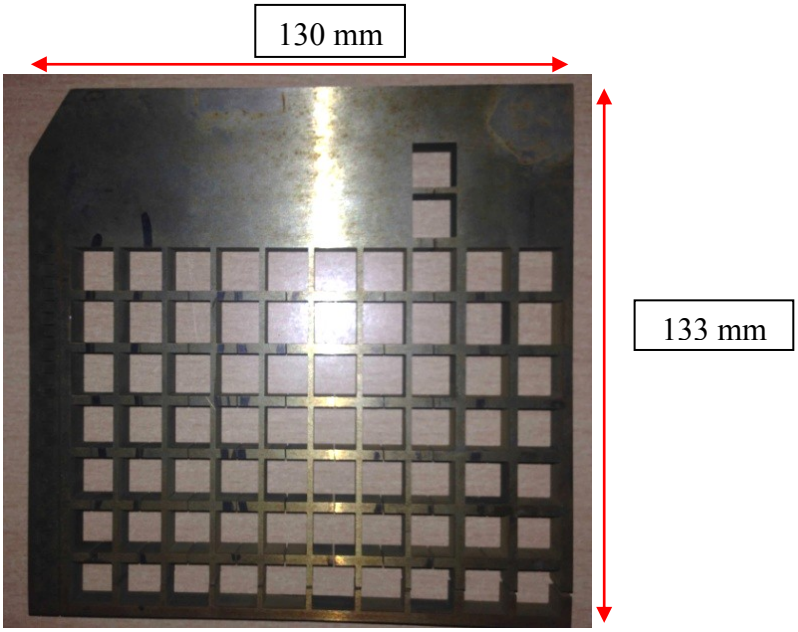

Figure 3.2: Dimensions of Workpiece, Thickness 10 mm

There are many types of wires used in the industries these days, which give better cutting rate and surface finish. But mostly brass wire (diameter =0.25 mm) is used in industries as well as in research work. Brass wire has high tensile strength as well as high electrical conductivity. Copper wires have high conductivity than brass but lesser tensile strength restricts their use in industries due to chances of breakage on high tension. Stratified wire or coated wires can also be used for better machining. According to literature review, very less work has been done by using stratified wires in WEDM process. So, two wires are used in this investigation and results for machining characteristics obtained with both wires are compared to study their influence on response values. Composition of wires used in experiments is described in Table 3.3 [Kern, 2007]. Figure 3.3 shows the wire spools.

Table 3.3 Types of Wires used in Experiment [Kern, 2007]

S. No.	Wire	Diameter (mm)	Composition	Melting Point	Tensile Strength
1.	Brass plain	0.25	Cu65% Zn35%	Brass- 920 ℃	900 N/mm^2
2.	Zinc Coated Brass	0.25	Core (Cu65% Zn35%) Coating (Zinc) 5µm	Brass- 920 ℃ Zinc coating- 419 ℃	900 N/mm^2

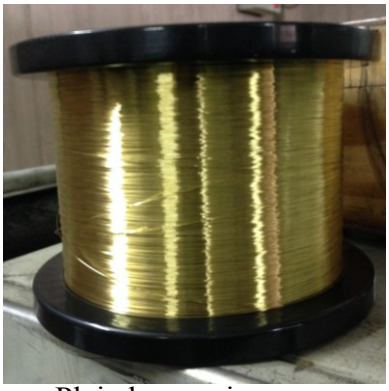

Plain brass wire

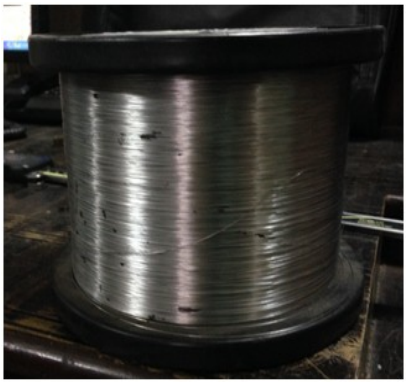

Zinc coated brass wire

Figure 3.3: Wire Spools [Photo Courtsey: Aman Metal Products, Ludhiana]

3.3 Measuring equipments and instruments

The various instruments and equipment used in this research work are discussed in this section.

3.3.1 Surftest SJ-400

Surftest SJ-400 is used to measure surface roughness of machined samples. The surface roughness is measured twice for three surface of each machined sample, i.e. total number of reading taken per sample is 6 and mean of these values is taken as final surface roughness for single sample. The average roughness (R_a) is generally used to measure surface roughness. R_a is measured by comparing all the peaks and valleys to the mean line, and then taking mean of all for the defined cut-off length i.e. 0.08 mm and stroke length of 4 mm. and rated in micron (μm). The Surftest SJ-400 equipment is shown in fig. 3.4.

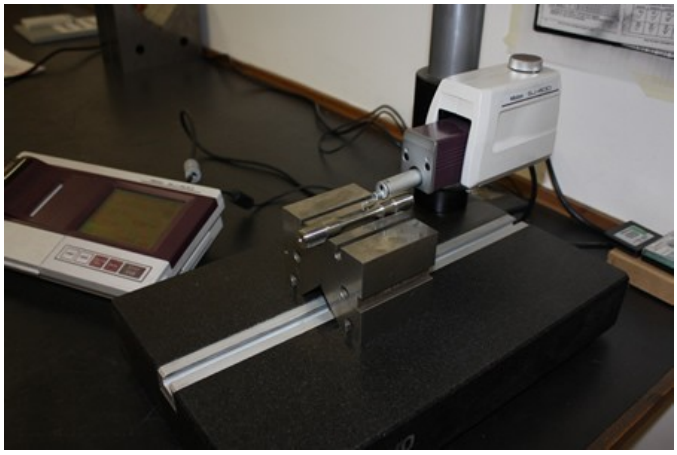

Figure 3.4: Surftest SJ-400 roughness tester [Photo Courtesy: Thapar university campus, Patiala]

3.3.2 Micro Hardness Tester

Hardness of the workpiece is examined by Micro Hardness tester. Hardness is calculated in Vickers scale to verify hardness property of the material procured with standard data available.

Figure 3.5 Micro Hardness Tester [Photo Courtesy: Thapar university campus, Patiala]

3.3.3 Spectrometer

Spectrometry technique is used to identify the amount and type of chemicals present in the D2 steel workpiece. The results for chemical composition obtained by microscopy are verified with the standard composition for D2 steel.

Figure 3.6 Spectrometer [Photo Courtesy: Thapar university campus, Patiala]

3.3.4 Profile Projector

Nikon Profile Projector V-10A is used to measure kerf width. Kerf width is calculated by measuring width of cut on the workpiece. Four reading are taken for each width of cut for a length of 5 mm. The least count of profile projector is 0.001 mm. Figure 3.7 shows the images of Profile Projector.

Figure 3.7: Nikon Profile Projector [Photo Courtesy: Thapar university campus, Patiala]

3.3.5 SEM & EDX

Scanning Electron Microscope technique is used to examine surface characteristics of machined sample. SEM is used to calculate white layer thickness and microstructure of machined specimen. The EDX technique is used to examine addition of chemical elements from wire or dielectric to workpiece surface. Figure 3.8 shows the image of SEM machine.

Figure 3.8: Mitutoyo Scanning Electron Microscope [Photo Courtesy: Thapar university campus, Patiala]

3.4 Preparation of Specimens

The D2 steel plate of 133 mm × 130 mm × 10 mm size is fixed in the saddle is shown in Fig. 3.9 on the Electronica Sprintcut WEDM Machine Tool and specimen of 10 mm × 10 mm × 10 mm size are machined. All set of machined specimens are shown in Fig. 3.10.

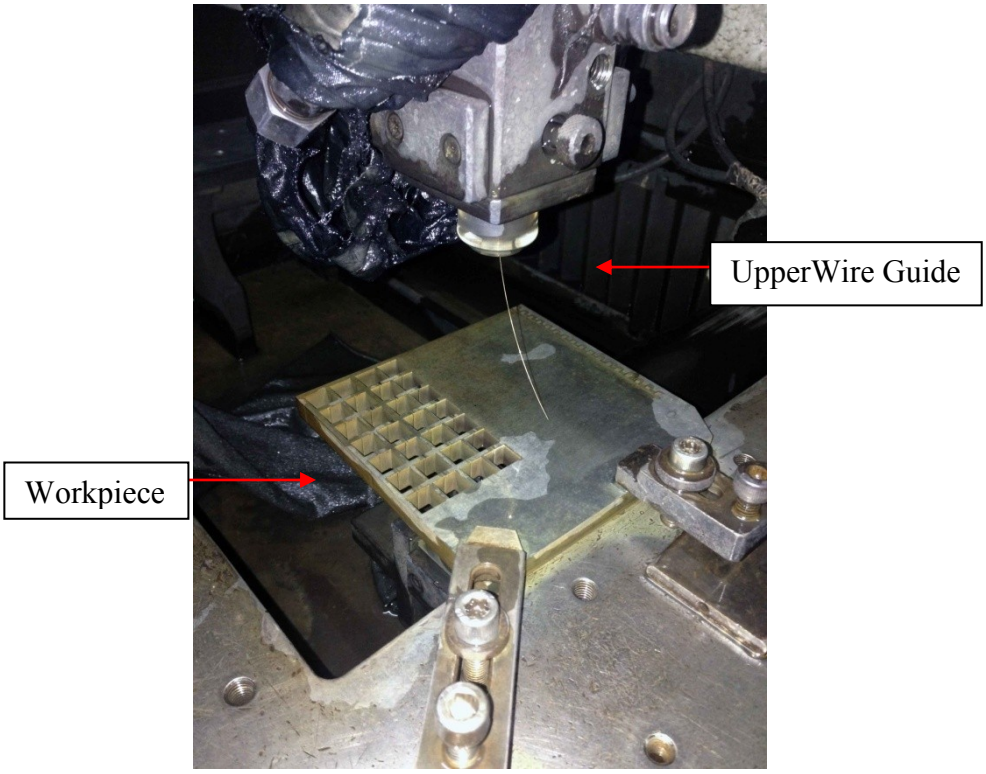

Figure 3.9: View of workpiece clamped on WEDM table

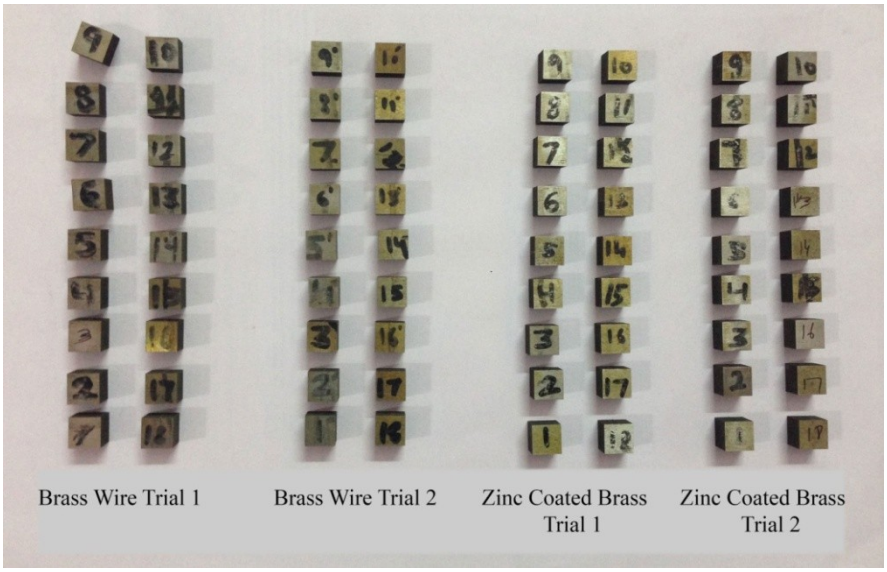

Figure 3.10: Machined Specimen (72) size 10mm*10mm*10mm

3.5 Pilot Study

The objective of the pilot experimentations is to examine the influence of different levels of various process variables on machining characteristics. Various machining performance characteristics in WIRE EDM are material removal rate (MRR) or cutting rate, surface roughness (SR) and dimensional deviation. It shows some trends in the results by which the parameters and their levels can be selected for the main investigation. The influence of input parameters is studied on cutting rate by varying one factor at a time (OFAT). The value of parameters which are kept constant is taken as the middle value of the range of respective factor and value of peak current is taken as highest value.

The pilot investigation was executed on ELEKTRA SPRINTCUT WEDM. In this pilot study different input parameters were varied (one factor a time approach). These include Pulse On Time (T_{ON}), Pulse Off Time (T_{OFF}), Peak Current (I_P), Servo Voltage (S_V), Wire Tension (W_T), Wire Speed (W_F). Table 3.4 shows the parameters which are kept constant at a fixed value during pilot study.

Table 3.4: Constants parameters for pilot study

Sr. No.	Factor	Fixed Value
1	Workpiece Material	D2 Alloy Steel (Hardened)
2	Cutting Tool	Brass Wire (Diameter- 0.25mm)
3	Workpiece Height	10 mm
4	Flushing Pressure	1 unit (15 kgf)
5	Peak Voltage	2 unit (110 V)
6	Dielectric Conductivity	20 Siemens
7	Servo Feed	2100

In pilot investigation, the workpiece is cut for 10 mm in a straight cut. The cutting rate is obtained from the display screen. The level of parameter is changed after 10 mm of cut and five reading of cutting speed are taken and mean of all reading is taken as final reading for specified level of the factor. This procedure is repeated for each factor.

3.5.1 Effect of Pulse on Time (T_{ON}) on Cutting Rate

The levels of pulse on time are selected in the range of 0.3 µs to 1.5 µs in steps of 0.15 microseconds. Table 3.5 shows values of other constant parameters Table 3.6 demonstrates the variation obtained in cutting rate when pulse on time is increased and it shows that the cutting rate increases with increase in T_{ON}. Figure 3.11 shows cutting rate increase in a straight line trend with the increase in T_{ON}.

Table 3.5: Constant parameters for Pulse on time vs. Cutting speed

Peak Current	Pulse off time	Spark gap voltage	Wire tension	Wire feed
230 A	26 µs	20 V	1140 g	8 m/min

Table 3.6: Pulse on time vs. Cutting Speed

S. No.	T_{ON} (µs)	Cutting Speed (mm/min)
1	0.30	1.09
2	0.45	1.34
3	0.60	1.51
4	0.75	1.87
5	0.90	2.45
6	1.05	2.72
7	1.20	3.29
8	1.35	3.4
9	1.50	3.56

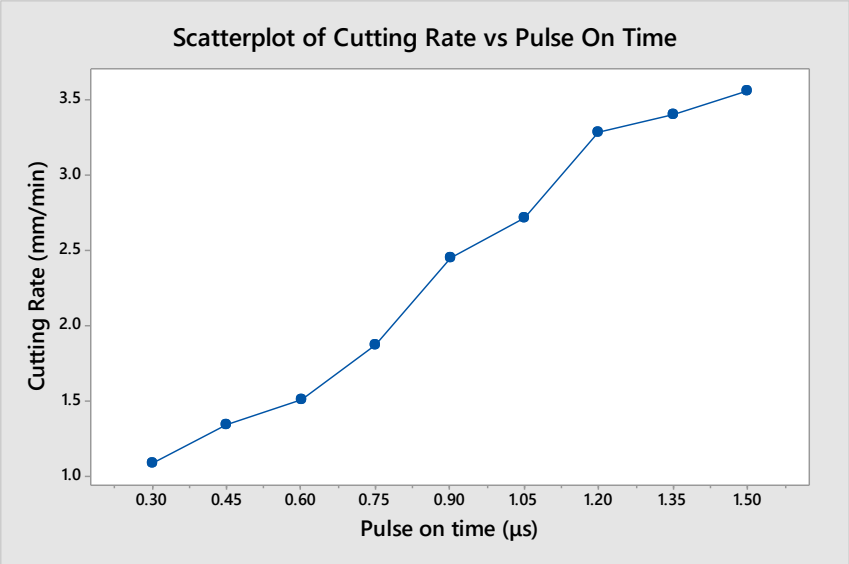

Figure 3.11: Cutting Rate vs. Pulse on time

3.5.2 Effect of Pulse off Time (T_{OFF}) on Cutting rate

In the next stage of study, the values of pulse time off (T_{OFF}) were selected from range 17 µs to 46 µs. Table 3.7 shows values of other constant parameters. The variation in cutting rate of material by changing pulse off time is presented in Table 3.8. Figure 3.12 shows the main effect plot of pulse off time versus cutting rate. The cutting rate decrease with increase in T_{OFF}. Figure 3.12 shows the decreasing trend of cutting rate with increase in T_{OFF}.

Table 3.7: Constant parameters for Pulse off time vs. Cutting speed

Peak Current	Pulse on time	Spark gap voltage	Wire tension	Wire feed
230 A	0.6 µs	20 V	1140 g	8 m/min

Table 3.8: Cutting Rate vs. Pulse off time

S. No.	T_{off} (µs)	Cutting Speed (mm/min)
1	17	2.62
2	19	2.53
3	22	2.32
4	26	2.12
5	30	2.03
6	34	1.89
7	38	1.71
8	42	1.46
9	46	1.23

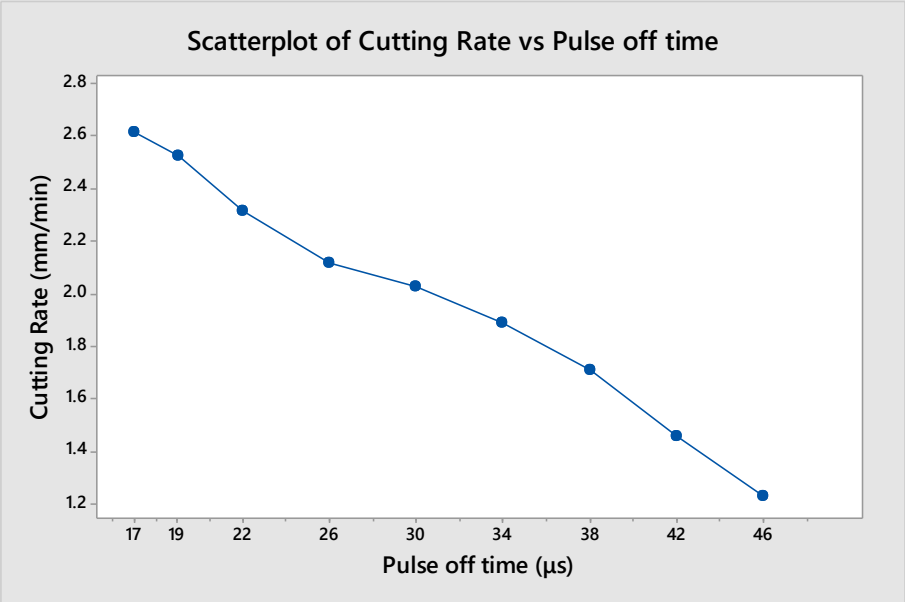

Figure 3.12: Cutting Rate vs. Pulse off time

3.5.3 Effect of Peak Current (I_p) on Cutting rate

The third set of experimentation describes that increasing Peak Current (I_p) results in rise of material removal rate. The values of constant process variables are shown in Table 3.9. Table 3.10 describes the variation in cutting rate due to change in I_p. Figure 3.13 shows the scatter plot of peak current versus cutting rate. The cutting rate increases with increase in I_p.

Table 3.9: Constant parameters for Peak Current vs. Cutting speed

Pulse on time	Pulse off time	Spark gap voltage	Wire tension	Wire feed
0.6 µs	26 µs	20 V	1140 g	8 m/min

Table 3.10: Cutting Rate vs. Peak Current

S. No.	I_p (ampere)	Cutting Speed (mm/min)
1	130	1.59
2	140	1.64
3	150	1.69
4	160	1.75
5	170	1.80
6	180	1.86
7	190	1.91
8	200	1.97
9	210	2.02
10	220	2.08
11	230	2.17

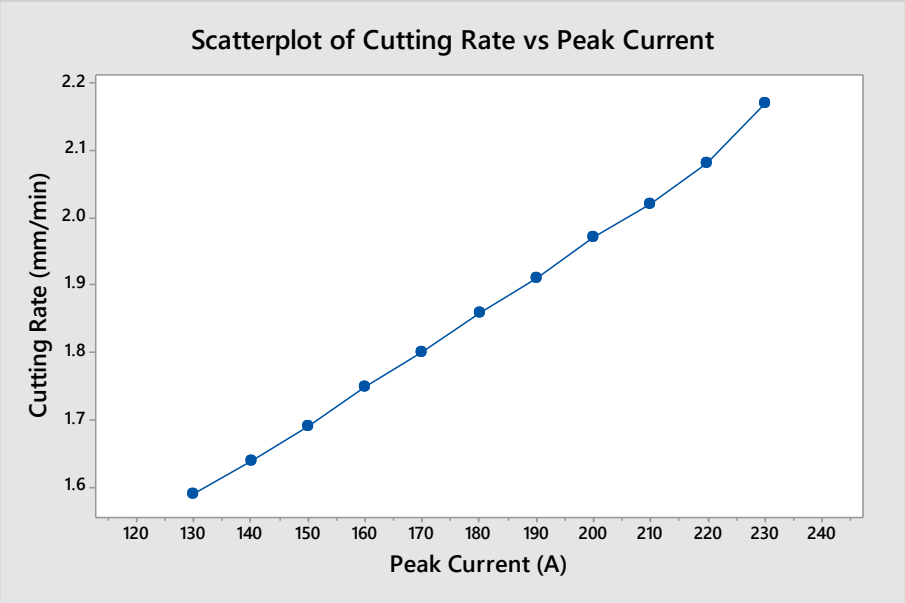

Figure 3.13: Cutting Rate vs. Peak Current

3.5.4 Effect of Spark Gap Set Voltage (S_V) on Cutting rate

The Servo Voltage was selected in the range of 15 volt to 45 volt. Table 3.11 shows the variation in cutting rate due to change in S_V. Table 3.8 shows values of other constant parameters. Figure 3.14 shows the scatter plot of servo voltage versus cutting rate. The cutting rate decreases with increase in S_v. Figure 3.14 shows the decreasing trend for cutting rate.

Table 3.11: Constant parameters for Spark Gap voltage vs. Cutting speed

Peak Current	Pulse on time	Pulse off time	Wire tension	Wire feed
230 A	0.6 µs	26 µs	1140 g	8 m/min

Table 3.12: Cutting Rate vs. Spark Gap set voltage

S. No.	S_V (volt)	Cutting Speed (mm/min)
1	15	2.22
2	20	2.13
3	25	2.08
4	30	2.01
5	35	1.95
6	40	1.87
7	45	1.79

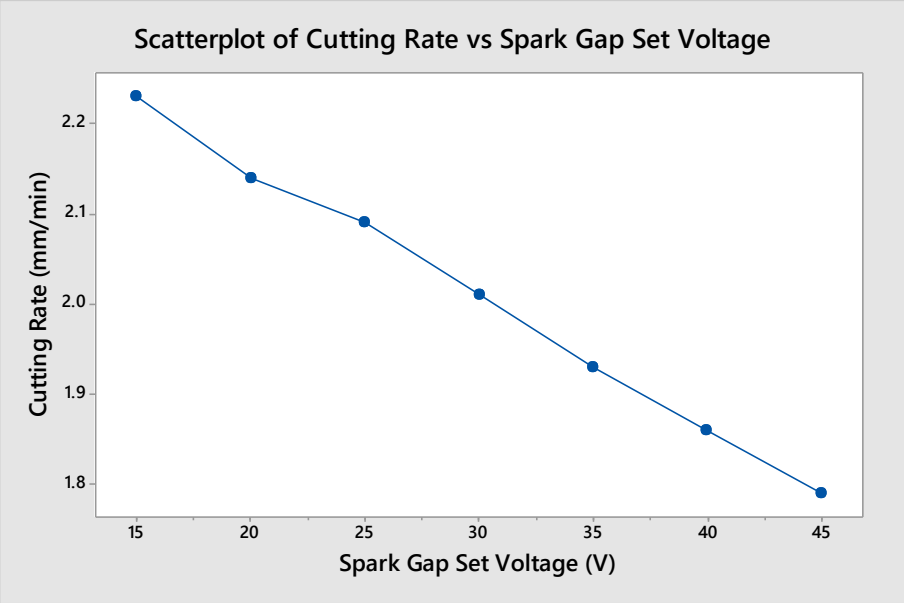

Figure 3.14: Cutting Rate vs. Spark Gap set voltage

3.5.5 Effect of Wire Tension (W_T) on Cutting rate

In the fifth set of experimentation the Wire Tension (W_T) was varied in the range of 420 grams to 1620 grams. Table 3.13 shows values of other constant parameters. Table 3.14 represents data obtained for cutting rate with change in wire tension. Figure 3.15 shows the scatter plot of wire tension versus cutting rate. The cutting rate remains constant with increase in W_T.

Table 3.13: Constant parameters for Wire Tension vs. Cutting speed

Peak Current	Pulse on time	Pulse off time	Spark gap voltage	Wire feed
230 A	0.6 µs	26 µs	20 V	8 m/min

Table 3.14: Cutting Rate vs. Wire Tension

S. No.	W_T (grams)	Cutting Speed (mm/min)
1	420	2.15
2	660	2.16
3	900	2.14
4	1140	2.14
5	1380	2.13
6	1620	2.14

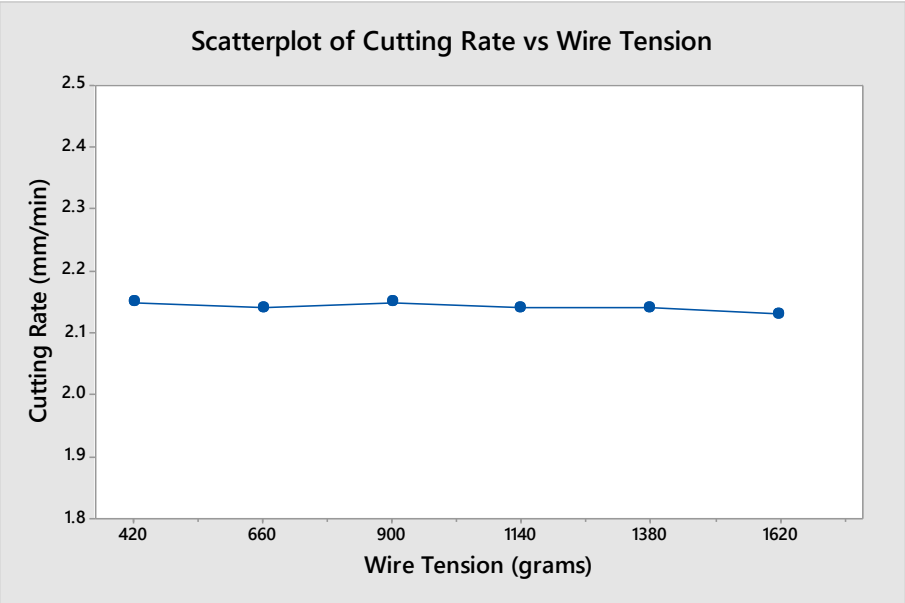

Figure 3.15: Cutting Rate vs. Wire Tension

3.5.6 Effect of Wire Feed (W_F) on Cutting rate

In the sixth and last set of experimentation the Wire Feed (W_F) was varied in the range of 2 m/min to 12 m/min. Table 3.15 shows the values of other constant parameters. Table 3.16 represents cutting rate when wire feed was varied individually. Figure 3.16 shows the scatter plot of wire feed versus cutting rate. The cutting rate remains constant with increase in W_F.

Table 3.15: Constant parameters for Wire Feed vs. Cutting speed

Peak Current	Pulse on time	Pulse off time	Spark gap voltage	Wire tension
230 A	0.6 µs	26 µs	20 V	1140 g

Table 3.16: Cutting Rate vs. Wire Feed

S. No.	W_F (m/min)	Cutting Speed (mm/min)
1	2	2.15
2	4	2.14
3	6	2.15
4	8	2.14
5	10	2.13
6	12	2.15

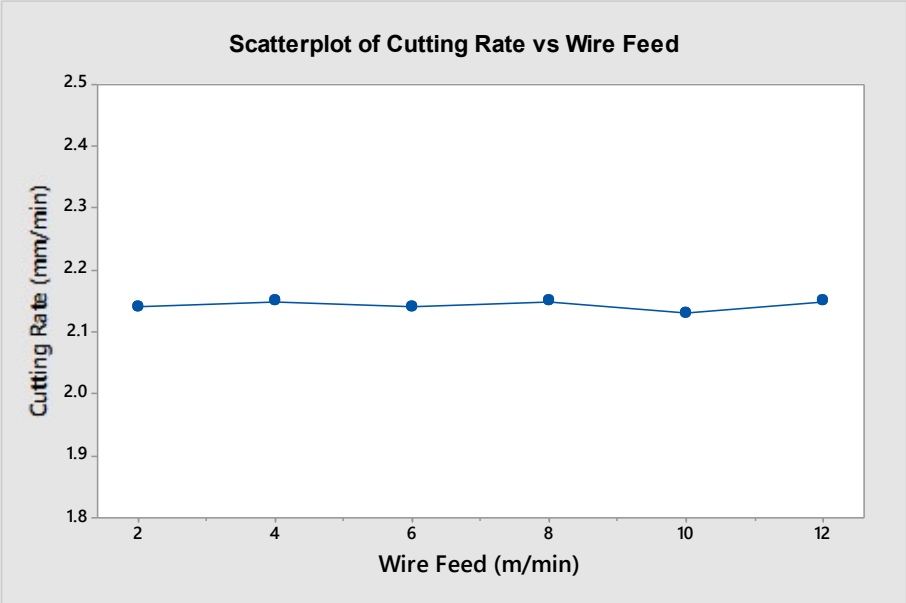

Figure 3.16: Cutting Rate vs. Wire Feed

3.6 Taguchi Method

3.6.1 Design of experiment

This section describes the process for designing, conducting and analyzing the experiments. In design of experiment, the layout for experimentation is designed. Accordingly, proper design and methodology is prepared and it estimates the number of experiments to be done to get the required results. After designing, conducting experiment is a major part of manufacturing process. This is followed by analyzing the experimental results to find the quality of machining and concluding the part of experimentation. Thus, the purpose of the whole research or study is emphasised in this section to achieve our goal.

i. Selection of factors to be evaluated

There are several useful methods for determining selection of factors in experiments. These are brainstorming, pilot experiments, and literature review and personnel experience. In this work, pilot study on parameters have been carried out by varying one factor at a time and the factors effecting machining characteristic are included in the main experimental study.

ii. Selection of number of levels of the factor

The degree of freedom can be defined as subtraction of 1 from number of levels (number of levels – 1). If levels are large then total degree of freedom in the experiment will increase which leads to increase in total number of test to be conducted. So, number of levels should be selected according to need so that number of total experiments remains within performing limit.

iii. Selection of the appropriate Orthogonal Array (OA)

The selection of OA depends upon:

- The number of factors of interest
- The number of levels for the factors of interest.

Orthogonal Arrays

The different types of OA's are as follows:

Fixed level design

- 2-level array- L4,L8,L12,L16,L32
- 3-level array- L9,L18,L27
- 4-level array- L16
- 5-level array- L25

Mixed level design

- Mixed 2-3 level array- L18,L36,L54
- Mixed 2-4 level array- L8,L16,L32
- Mixed 2-8 level array- L16
- Mixed 3-6 level array- L18

In this study, number of factors and levels are considered according to pilot study which was stated earlier in this report. The significant factors considered are based on their effect on machining parameters. Levels are considered by personnel experience and literature review. Taguchi's L18 OA is used for the design of experiment and consisted of 4 parameters with mixed 6-3 levels.

iv. Assigning factors and interactions to the column

This is an important step of a design of experiment which consist interactions within the main factors. Taguchi's OA stated various rules for assigning the main factors and interaction to columns of OA. Linear Graphs and triangular tables are used to assign to factors and interactions to different columns.

v. Conduct tests

The preparation for performing experiments can begin if the factors are assigned to columns of an Orthogonal Array. Experiments can be done according to the OA and further statistical analysis will give the results. The L18 (mixed 6-3 level) OA is shown in table 3.17.

Table 3.17: L18 4- factors (mixed 6-3 level)

Trial Number	A	B	C	D
1	1	1	1	1
2	1	2	2	2
3	1	3	3	3
4	2	1	1	2
5	2	2	2	3
6	2	3	3	1
7	3	1	2	1
8	3	2	3	2
9	3	3	1	3
10	4	1	3	3
11	4	2	1	1
12	4	3	2	2
13	5	1	2	3
14	5	2	3	1
15	5	3	1	2
16	6	1	3	2
17	6	2	1	3
18	6	3	2	1

3.6.2 Analysis of Experimental Results

Results are analyzed to find the effects of different machining performance parameters. An analysis of variance (ANOVA) and signal to noise (S/N) ratio techniques are used. Based on implementation of these techniques on the experimental results, optimum machining characteristics can be obtained by statistical analysis.

i. Calculation of S/N ratio

Taguchi has created a transmutation of repetition data to some other value which measure out deviations present in the experiments. The transformation is signal to noise (S/N) ratio. The S/N ratio, which condenses the multiple data points within a trial, depends on the type of characteristic being evaluated[*]. The equations for calculating the S/N ratios for lower the best, nominal the best and higher the best characteristics are:

- Lower the best- The S/N_{LB} is used for situations where the target value is zero, such as surface roughness. Eq. (3.1) defines calculation for lower the best S/N ratio.

$$S/N_{LB} = -10 \log \left[\left(\frac{1}{r}\sum_{i=1}^{r} y^2\right)\right] \quad (3.1)$$

- Larger the best- It is used when the largest value is desired, such as MRR. Eq. (3.2) describes the formula for calculating higher the best characteristics.

$$S/N_{HB} = -10 \log \left[\frac{1}{r} \sum_{i=1}^{r} \frac{1}{y2} \right] \quad (3.2)$$

* A Higher S/N ratio is required for better performance.

ii. Analysis of Variance and F-test

ANOVA is a numerical method which divides total deviation down into answerable sources. The total deviation is disintegrating into its appropriate components. ANOVA is a statistical decision tool for sleuthing any gaps in average interpretation of groups of factors tested. This total sum of squared deviation (SS_T) can be decomposed into two components i.e. the sum of squared deviation due to each process parameters (SS_D) and the sum of squared errors (SS_e). The percentage contribution is the ratio of (SS_D) to (SS_e). The significant effect of each parameter can be identified by F-test. It is the ratio of the mean of squared deviation (SS_m) to the mean of squared error (SS_{em}). SS_m is equal to the sum of the squared deviation (SS_d) divided by the number of degree of freedom associated with the process parameter.

3.6.3 Confirmation experiment

The verification experiment is the concluding step in confirming the conclusions. The best conditions are set for the significant factors and levels. Various trials are made under invariant conditions. The mean of the confirmation experiment results is equated to the expected mean based on the factors and levels tested.

Chapter 4

Results and Analysis

4.1 Introduction

As mentioned in the previous chapters, the experimentations are carried out based on dhe present chapter which describes the application of the Taguchi experimental design methodology. The strategy for main investigation part was selected and according to design, the experiments were conducted. The influences of process variables on the response characteristics were analyzed. The response parameters are material removal rate, surface roughness and kerf width. The plain brass wire and zinc coated brass wire are used for the experimentation and results are compared to get the optimum machining characteristics. The results are discussed subsequently in the following sections.

4.1.1 Selection of Orthogonal array and parameters assignment

This section describes the selection of four process parameters and their levels. Minimum levels for parameters selected are three to find true influence of parameters on response characteristics. One parameter is varied to six levels to examine its effect for wide range. So the orthogonal array is selected in such a way that OA should have minimum 3 level of factor. Mixed level OA is used in the present work with 1 factor at 6 levels and other 3 factors at 3 levels. The parameters selected with their level values are given in table 4.1.

Table 4.1 Selected Process parameters for experiments

Factors	Parameters (Units)		Levels					
			1	2	3	4	5	6
A	I_P	Peak Current (A)	130	150	170	190	210	230
B	T_{ON}	Pulse on time (µs)	0.6	0.9	1.2	-	-	-
C	T_{OFF}	Pulse Off Time (µs)	19	26	34	-	-	-
D	S_V	Spark Gap Set Voltage (V)	20	30	40	-	-	-

According to Taguchi design method, a set of mixed 6-3 levels, first factor has 6 levels and has five degrees of freedom (DOF) and other three factors are assigned 3 levels,

each having two degrees of freedom. Total DOF becomes 11 for four process parameters. Total DOF for the OA are 17 i.e. 18-1. Table 4.2 shows the L18 OA with levels assigned to each experimental run. Two trials of experiment are done for each experiment run.

Table 4.2: L18 Mixed (6-3 level) orthogonal Array with 4 Factors

Trial No.	I_p	T_{on}	T_{off}	S_v
1	1	1	1	1
2	1	2	2	2
3	1	3	3	3
4	2	1	1	2
5	2	2	2	3
6	2	3	3	1
7	3	1	2	1
8	3	2	3	2
9	3	3	1	3
10	4	1	3	3
11	4	2	1	1
12	4	3	2	2
13	5	1	2	3
14	5	2	3	1
15	5	3	1	2
16	6	1	3	2
17	6	2	1	3
18	6	3	2	1

4.2 Experimental Results

The trial results are investigated to find influence of process variables on response characteristics. Table 4.3 indicates the general overview of actual values of parameters assigned to each run. Mean and S/N ratio of the experimental results for material removal rate and surface roughness are given in Table 4.4 and kerf width is shown in Table 4.5 for plain brass wire. Table 4.6 shows mean and S/N ratio values of material removal rate and surface roughness and Table 4.7 shows for kerf width by zinc coated brass wire. 18 trials of experimentation were executed according to Taguchi experimental design methodology. Each experiment was repeated twice, R1, R2, represent response values for two repetitions of each trial for obtaining S/N values and with two wires; brass and zinc coated brass. Total number of experiments performed is 72. In this research work, all the designs, scatter-plots diagrams and analysis is carried out using Minitab 17 statistical software.

Table 4.3: L18 OA with process parameter values

Column No.	1	2	3	4	Responses		S/N Ratio
Trial No.	I_P	T_{on}	T_{off}	S_v	R1	R2	
1	130	0.6	19	20			
2	130	0.9	26	30			
3	130	1.2	34	40			
4	150	0.6	19	30			
5	150	0.9	26	40			
6	150	1.2	34	20			
7	170	0.6	26	20			
8	170	0.9	34	30			
9	170	1.2	19	40			
10	190	0.6	34	40			
11	190	0.9	19	20			
12	190	1.2	26	30			
13	210	0.6	26	40			
14	210	0.9	34	20			
15	210	1.2	19	30			
16	230	0.6	34	30			
17	230	0.9	19	40			
18	230	1.2	26	20			

The experiments were executed on WEDM by varying different levels (defined earlier in this chapter) for different parameters. The Taguchi's parametric approach gives the mean value and signal to noise ratio (S/N) of the machining characteristics for each factor at different levels. The influences of process variables on the selected performance parameters are discussed. The process parameters are material removal rate (MRR), kerf width and surface roughness (SR). The main effects diagrams of process parameters for mean data and signal to noise ratio data are plotted. The parametric effects are examined by response curves. Significant variables are identified by using analysis of variance (ANOVA) and S/N ratio technique for raw data. These techniques are used to measure influence of process parameters on the machining characteristics. The experimental data given in Tables 4.4 and 4.5 shows the response values for MRR, surface roughness and kerf for plain brass wire. Table 4.6 and 4.7 shows the experimental data for zinc coated brass wire for MRR, surface roughness and kerf. The experimental data represent the mean values and S/N values for each performance characteristics.

Table 4.4: Response Data- Plain Brass Wire (MRR & SR)

MRR (mm^3/min)				S/N Ratio (db)	Surface Roughness(μm)				S/N Ratio (db)
Trial No.	R1	R2	Mean		Trial No.	R1	R2	Mean	
1	4.39	4.46	4.43	12.92	1	2.83	2.63	2.73	-8.71
2	6.01	5.96	5.99	15.54	2	2.91	2.75	2.83	-9.03
3	5.91	5.88	5.90	15.41	3	2.73	3.13	2.93	-9.36
4	4.32	4.39	4.36	12.78	4	2.57	2.58	2.57	-8.20
5	5.57	5.54	5.56	14.89	5	2.73	2.61	2.67	-8.54
6	7.49	7.61	7.55	17.56	6	3.21	3.28	3.24	-10.22
7	3.66	3.72	3.69	11.34	7	2.60	2.52	2.56	-8.16
8	4.87	4.92	4.90	13.79	8	2.39	2.57	2.48	-7.88
9	8.75	8.67	8.71	18.80	9	3.51	3.15	3.33	-10.46
10	2.79	2.82	2.81	8.96	10	1.67	1.60	1.63	-4.27
11	7.80	7.82	7.81	17.85	11	2.94	3.03	2.99	-9.50
12	9.13	9.06	9.10	19.18	12	3.27	3.26	3.26	-10.27
13	3.29	3.31	3.30	10.37	13	1.93	1.89	1.91	-5.61
14	5.85	5.97	5.91	15.43	14	2.66	2.77	2.71	-8.67
15	8.56	8.64	8.60	18.69	15	3.62	3.18	3.40	-10.64
16	3.12	3.17	3.15	9.95	16	2.23	2.28	2.25	-7.06
17	9.14	9.21	9.18	19.25	17	2.84	2.84	2.84	-9.06
18	10.03	9.91	9.97	19.97	18	3.53	3.45	3.49	-10.86

Table 4.5: Response Data- Plain Brass Wire (Kerf width)

Kerf Width (mm)				S/N Ratio (db)
Trial No.	R1	R2	Mean	
1	0.263	0.265	0.264	11.57
2	0.276	0.280	0.278	11.12
3	0.274	0.272	0.273	11.28
4	0.262	0.263	0.263	11.62
5	0.270	0.271	0.271	11.36
6	0.281	0.279	0.280	11.06
7	0.258	0.260	0.259	11.73
8	0.267	0.267	0.267	11.47
9	0.299	0.301	0.300	10.46
10	0.259	0.259	0.259	11.73
11	0.291	0.295	0.293	10.66
12	0.307	0.311	0.309	10.20
13	0.259	0.261	0.260	11.70
14	0.275	0.276	0.276	11.20
15	0.299	0.303	0.301	10.43
16	0.261	0.261	0.261	11.67
17	0.311	0.313	0.312	10.12
18	0.327	0.330	0.329	9.67

Table 4.6: Response Data- Zinc coated Brass wire (MRR & SR)

MRR (mm^3/min)				S/N Ratio (db)	Surface Roughness(μm)				S/N Ratio (db)
Trial No.	R1	R2	Mean		Trial No.	R1	R2	Mean	
1	4.73	4.93	4.83	13.67	1	2.52	2.43	2.47	-7.87
2	7.84	7.87	7.85	17.90	2	2.52	2.71	2.61	-8.34
3	8.10	7.97	8.04	18.10	3	2.75	2.76	2.75	-8.79
4	5.78	5.91	5.84	15.33	4	2.38	2.31	2.34	-7.40
5	7.42	7.64	7.53	17.54	5	2.54	2.42	2.48	-7.89
6	8.46	9.94	9.20	19.19	6	3.06	3.02	3.04	-9.66
7	4.58	5.07	4.82	13.63	7	2.37	2.26	2.32	-7.29
8	6.73	7.01	6.87	16.73	8	2.43	2.40	2.41	-7.65
9	12.16	12.25	12.21	21.73	9	3.09	3.11	3.10	-9.82
10	3.61	3.64	3.63	11.19	10	1.91	1.80	1.85	-5.36
11	8.30	8.10	8.20	18.27	11	2.53	2.65	2.59	-8.28
12	9.45	9.37	9.41	19.47	12	2.96	2.91	2.94	-9.35
13	4.53	4.64	4.58	13.22	13	2.00	1.92	1.96	-5.84
14	7.56	7.62	7.59	17.60	14	2.50	2.52	2.51	-7.99
15	10.72	10.59	10.65	20.55	15	3.12	3.09	3.10	-9.83
16	4.59	4.47	4.53	13.12	16	2.19	2.08	2.13	-6.59
17	12.16	12.01	12.09	21.64	17	2.51	2.43	2.47	-7.86
18	10.44	10.79	10.61	20.51	18	2.94	2.98	2.96	-9.43

Table 4.7: Response Data- Zinc coated Brass Wire (Kerf width)

Kerf Width (mm)				S/N Ratio (db)
Trial No.	R1	R2	Mean	
1	0.277	0.270	0.274	11.26
2	0.289	0.295	0.292	10.69
3	0.283	0.289	0.286	10.87
4	0.273	0.270	0.272	11.32
5	0.280	0.284	0.282	10.99
6	0.290	0.300	0.295	10.60
7	0.264	0.271	0.268	11.45
8	0.285	0.294	0.290	10.77
9	0.311	0.319	0.315	10.03
10	0.272	0.266	0.269	11.40
11	0.316	0.312	0.314	10.06
12	0.325	0.335	0.330	9.63
13	0.279	0.283	0.281	11.03
14	0.292	0.287	0.290	10.77
15	0.315	0.320	0.318	9.96
16	0.279	0.276	0.278	11.13
17	0.330	0.325	0.328	9.70
18	0.340	0.346	0.343	9.29

4.2.1 Effect on MRR with Brass Wire

Figures 4.1 and 4.2 shows graphically that the MRR tends to rise with an increase in value of pulse on time and it also shows that with increasing pulse off time and spark gap voltage, MRR drops. Discharge energy is a function of current and pulse duration. The investigation shows as pulse duration and current intensity increases, the formation of high impulsive discharge energy increases the MRR. The number of discharges increases as pulse off time decreases which leads to a higher material removal rate. With increase in spark gap voltage the average discharge gap as well as discharge waiting time increases resulting into slow cutting process. MRR shows a varying trend with respect to peak current, it first increases then decreases and shows similar pattern for rest levels and in the end it increases to a high value at high value of I_P.

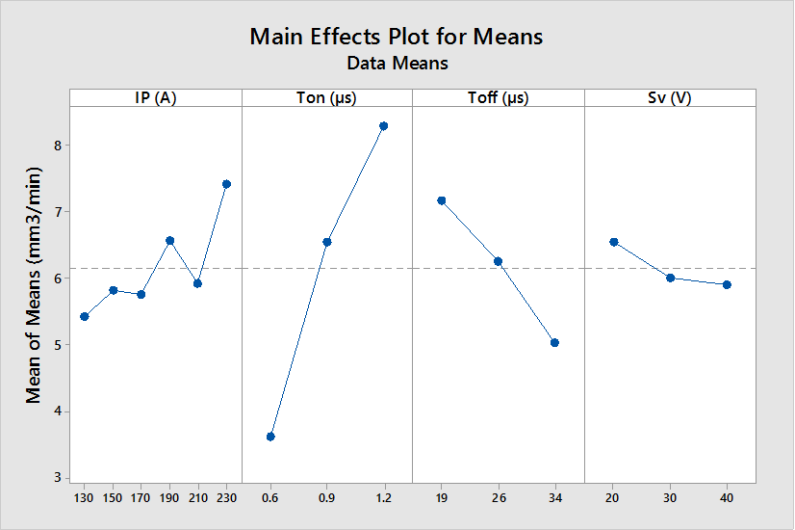

Figure 4.1: Main Effects Plot for Means MRR (Brass Wire)

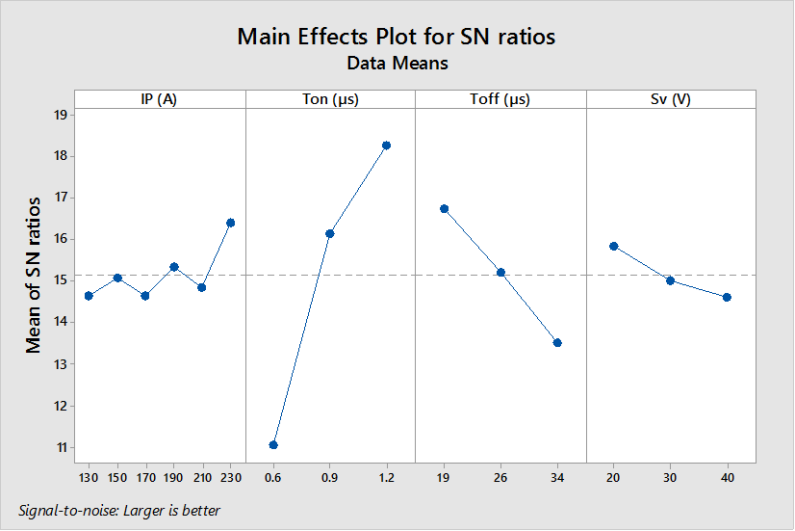

Figure 4.2: Main Effects Plot for SN ratios MRR (Brass Wire)

According to delta statistics described in Table 4.8 & 4.9, ranks are assigned to the factors as per their significance value. The delta value is obtained by subtracting smaller value from the larger value for each factor and ranks are assigned accordingly. Highest delta value got the highest rank. The MRR is higher the better characteristic.

Table 4.8: Response Table for MRR S/N Ratios (Brass Wire)

Level	I_P	T_{on}	T_{off}	S_v
1	14.62	11.05	16.72	15.85
2	15.08	16.13	15.22	14.99
3	14.64	18.27	13.52	14.61
4	15.33	-	-	-
5	14.83	-	-	-
6	16.39	-	-	-
Delta	1.77	7.22	3.20	1.23
Rank	3	1	2	4

Table 4.9: Response Table for MRR Means (Brass Wire)

Level	I_P	T_{on}	T_{off}	S_v
1	5.435	3.620	7.179	6.559
2	5.820	6.55	6.266	6.013
3	5.765	8.303	5.033	5.907
4	6.570	-	-	-
5	5.937	-	-	-
6	7.430	-	-	-
Delta	1.995	4.683	2.146	0.653
Rank	3	1	2	4

Table 4.10 shows the significant effect of parameters. The factor with p-value less than .05 is counted significant due to 95% confidence level taken during analysis. The significant factors for mean MRR are T_{on} (72.7%), T_{off} (15.06%) and I_p (8.53%) and S_v is the least significant factor. The R^2 value obtained from the model is .9797 which means 97.97% of the variation is due to factors considered in this investigation and 2.03% variation is due to error or unexplained by the model. Table 4.11 shows ANOVA calculation for S/N values.

Table 4.10 ANOVA for MRR Mean (Brass wire)

Source	DoF	SS	MS	F- Value	P-value	% Cont.	Significance
I_P	5	7.884	1.5769	5.05	0.037	8.53	Significant
T_{ON}	2	67.209	33.6045	107.52	0.000	72.77	Significant
T_{OFF}	2	13.916	6.9578	22.26	0.002	15.06	Significant
S_V	2	1.472	0.7358	2.35	0.176	1.59	Insignificant
Error	6	1.875	0.3125	-	-	-	-
Total	17	92.356	-	-	-	-	-
Model Summary		S		R^2		R^2 (adj)	
		0.559044		97.97%		94.25%	

Table 4.11: ANOVA for MRR S/N Ratio (Brass wire)

Source	DoF	SS	MS	F- Value	P-value	% Cont.	Significance
I_P	5	6.649	1.3298	2.07	0.0372	3.15	Significant
T_{ON}	2	164.785	82.3923	128.29	0.000	78.17	Significant
T_{OFF}	2	30.722	15.3612	23.92	0.001	14.57	Significant
S_V	2	4.781	2.3907	3.72	0.089	2.27	Insignificant
Error	6	3.853	0.6422	-	-	-	-
Total	17	210.791	-	-	-	-	-
Model Summary		S		R^2		R^2 (adj)	
		0.801384		98.17%		94.82%	

4.2.2 Effect on Surface Roughness with Brass wire

It is seen from the Fig. 4.3 and Fig. 4.4 that surface roughness increases with the increase in pulse on time. There is a decrease in surface roughness when the value of pulse off time and spark gap set voltage increases. The discharge energy increases by increasing pulse on time and decreasing pulse off time. Lesser pulse off time, more often discharge will occur, results in unstable and more non-uniform MRR. This leads to generate large crater and surface roughness will increase. Increase in spark voltage increases gap between electrodes and results in widening of area for discharge and it decreases discharge intensity over small area. Hence, surface roughness decreases.

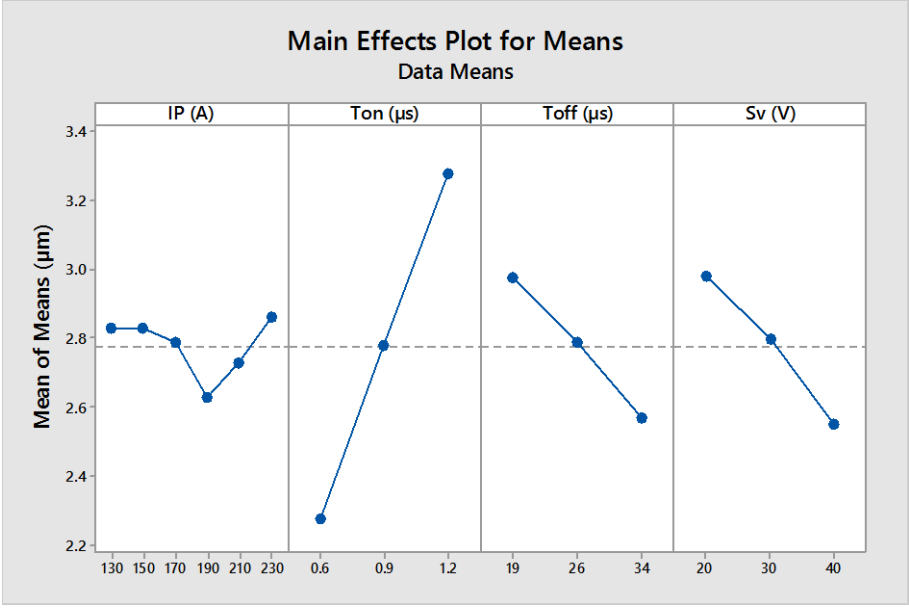

Figure 4.3 Main Effects Plot for SR Means (Brass Wire)

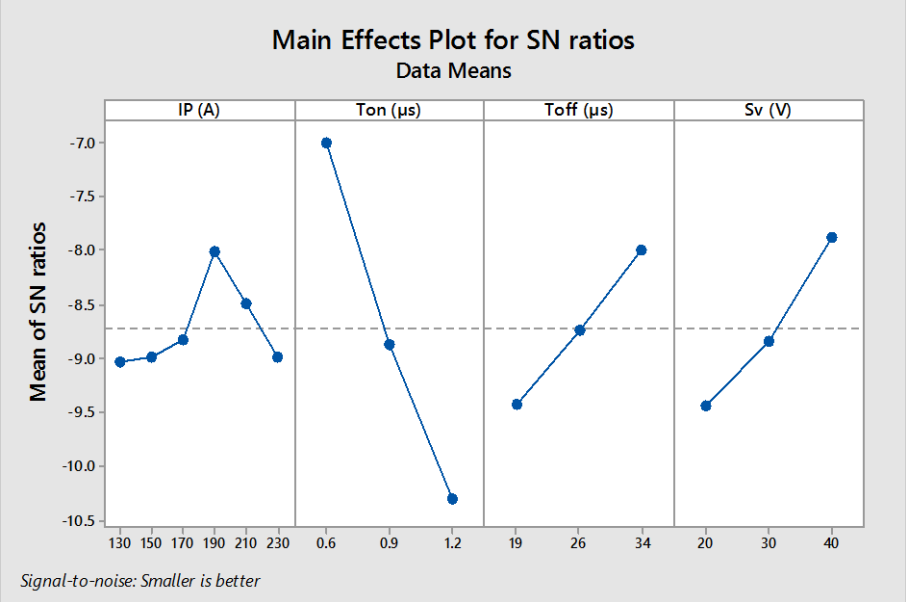

Figure 4.4: Main Effects Plot for SR S/N ratios (Brass Wire)

Table 4.12 & 4.13 illustrates the delta statistics and the ranks are assigned to the factors as per their significance value. Surface roughness is a lower the better performance characteristic.

Table 4.12: Response Table for SR S/N Ratios (Brass wire)

Level	I_P	T_{on}	T_{off}	S_v
1	-9.034	-6.996	-9.427	-9.352
2	-8.983	-8.777	-8.743	-8.846
3	-8.830	-10.300	-7.904	-7.875
4	-8.006	-	-	-
5	-8.307	-	-	-
6	-8.987	-	-	-
Delta	1.028	3.304	1.532	1.477
Rank	4	1	2	3

Table 4.13: Response Table for SR Means (Brass wire)

Level	I_P	T_{on}	T_{off}	S_v
1	2.828	2.174	2.973	2.952
2	2.828	2.751	2.786	2.798
3	2.787	3.275	2.440	2.550
4	2.626	-	-	-
5	2.672	-	-	-
6	2.859	-	-	-
Delta	0.233	1.001	0.433	0.402
Rank	4	1	2	3

The factor with p-value less than .05 is counted significant due to 95% confidence level taken during analysis. ANOVA table 4.14 shows the significant factors for mean surface roughness as T_{on} (70.53%), T_{off} (13.25%) and S_v (11.56%) and I_p is the least significant factor. The R^2 value obtained from the model is .9853 which means 98.53% of the variation is due to factors considered in this investigation and 1.47% variation is due to error or unexplained by the model. Table 4.15 shows ANOVA for S/N surface roughness values.

Table 4.14: ANOVA for Surface roughness Mean (Brass wire)

Source	DoF	SS	MS	F- Value	P-value	% Cont.	Significance
I_P	5	0.13518	0.02704	2.59	0.139	3.16	Insignificant
T_{ON}	2	3.00972	1.50486	144.26	0.000	70.53	Significant
T_{OFF}	2	0.56560	0.28280	27.11	0.001	13.25	Significant
S_V	2	0.49365	0.24682	23.66	0.001	11.56	Significant
Error	6	0.06259	0.01043	-	-	-	-
Total	17	4.26674	-	-	-	-	-
Model Summary		S		R^2		R^2 (adj)	
		0.102135		98.53%		95.84%	

Table 4.15: ANOVA for Surface roughness S/N Ratio (Brass wire)

Source	DoF	SS	MS	F- Value	P-value	% Cont.	Significance
I_P	5	2.730	0.5460	1.99	0.213	5.37	Insignificant
T_{ON}	2	32.68	16.340	59.69	0.000	64.31	Significant
T_{OFF}	2	6.882	3.4409	12.57	0.007	13.54	Significant
S_V	2	6.878	3.4392	12.56	0.007	13.54	Significant
Error	6	1.643	0.2738	-	-	-	-
Total	17	50.815	-	-	-	-	-
Model Summary		S		R^2		R^2 (adj)	
		0.523230		96.77%		90.84%	

4.2.3 Effect on Kerf Width with Brass Wire

It is seen from the Fig. 4.5 and Fig. 4.6 that kerf width tends to rise with the rise in pulse on time and peak current. It is found that width of cut decreases with increasing pulse off time. It has been seen that kerf is always greater than the diameter of the wire. The value of kerf width required is less as its large value affects the dimensional accuracy of cutting process. High pulse on time and low pulse off time increases the discharge energy results in high MRR and widen the width of cut. The peak current is least significant in case width of cut and greater the distance between electrodes lesser is the discharge intensity lesser the material erodes lesser will be kerf.

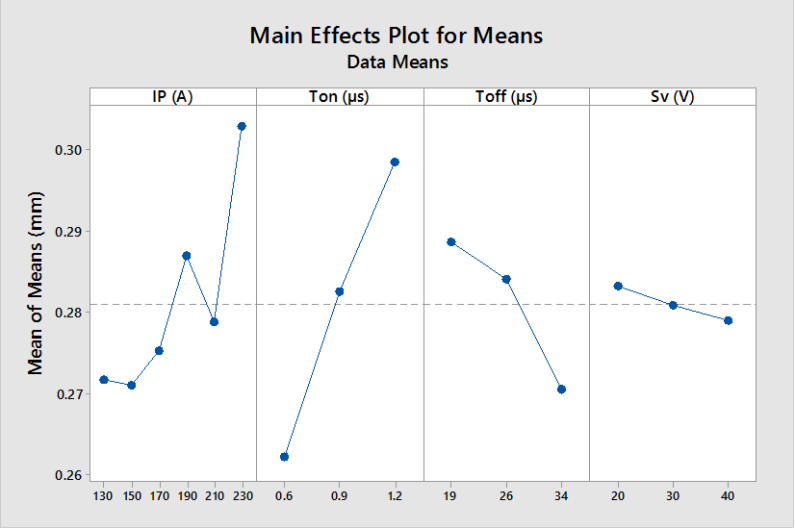

Figure 4.5: Main Effects Plot for Kerf Width Means (Brass Wire)

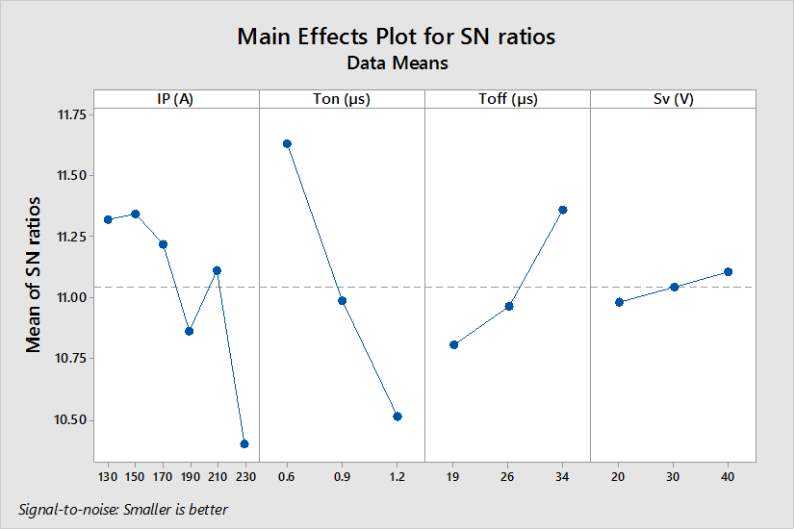

Figure 4.6: Main Effects Plot for Kerf Width S/N ratios (Brass Wire)

The delta value is obtained by subtracting smaller value from the larger value for each factor and ranks are assigned accordingly as shown in tables 4.16 & 4.17. Highest delta value got the highest rank.

Table 4.16: Response Table for Kerf S/N Ratios (Brass wire)

Level	I_P	T_{on}	T_{off}	S_v
1	11.32	11.67	10.81	10.98
2	11.34	10.99	10.96	11.08
3	11.22	10.51	11.40	11.11
4	10.87	-	-	-
5	11.11	-	-	-
6	10.48	-	-	-
Delta	0.86	1.16	0.59	0.13
Rank	2	1	3	4

Table 4.17: Response Table for Kerf Means (Brass wire)

Level	I_P	T_{on}	T_{off}	S_v
1	0.272	0.261	0.289	0.283
2	0.271	0.283	0.284	0.280
3	0.275	0.299	0.269	0.279
4	0.287	-	-	-
5	0.279	-	-	-
6	0.301	-	-	-
Delta	0.030	0.038	0.020	0.004
Rank	2	1	3	4

ANOVA Table 4.18 shows the significant factors for Kerf as T_{on} (53.24 T_{off} (14.40%) and I_p (29.70%) and S_v is the least significant factor. The R^2 value obtained from the model is .9806 which means 98.06% of the variation is explained by factors considered in this investigation and 1.94% variation is due to error or unexplained by the model. Table 4.19 shows ANOVA for kerf width S/N values.

Table 4.18: ANOVA for Kerf Mean (Brass wire)

Source	DoF	SS	MS	F- Value	P-value	% Cont.	Significance
I_P	5	0.002231	0.000446	18.35	0.001	29.70	Significant
T_{ON}	2	0.004000	0.002000	82.23	0.000	53.24	Significant
T_{OFF}	2	0.001082	0.000541	22.24	0.002	14.40	Significant
S_V	2	0.000054	0.000027	1.12	0.387	0.72	Insignificant
Error	6	0.000146	0.000024	-	-	-	-
Total	17	0.007513	-	-	-	-	-
Model Summary		S		R^2		R^2 (adj)	
		0.0049315		98.06%		94.50%	

Table 4.19: ANOVA for Kerf S/N Ratio (Brass wire)

Source	DoF	SS	MS	F- Value	P-value	% Cont.	Significance
I_P	5	1.6372	0.327	10.16	0.007	23.18	Significant
T_{ON}	2	4.0483	2.024	62.83	0.000	57.32	Significant
T_{OFF}	2	1.1306	0.565	17.55	0.003	16.01	Significant
S_V	2	0.0536	0.026	0.83	0.479	0.76	Insignificant
Error	6	0.1932	0.032	-	-	-	-
Total	17	7.0632	-	-	-	-	-
Model Summary		S		R^2		R^2 (adj)	
		0.179487		97.26%		92.25%	

4.2.4 Effect on MRR with Zinc Coated Brass wire

It is described in Fig. 4.7 and Fig. 4.8 that the material removal rate tends to rise with increasing pulse on time. It is found that MRR decreases with increasing pulse off time. The main reason behind this is long period of pulse on time. The high duration of current generates high intensity discharge energy which leads to large erosion of material. Pulse off

time also influences the MRR as its low value increases the frequency of discharge and results in high MRR. MRR shows a varying trend with respect to peak current, it first increases to three levels then decreases to one level, again increases to a high value at high value of I_P.

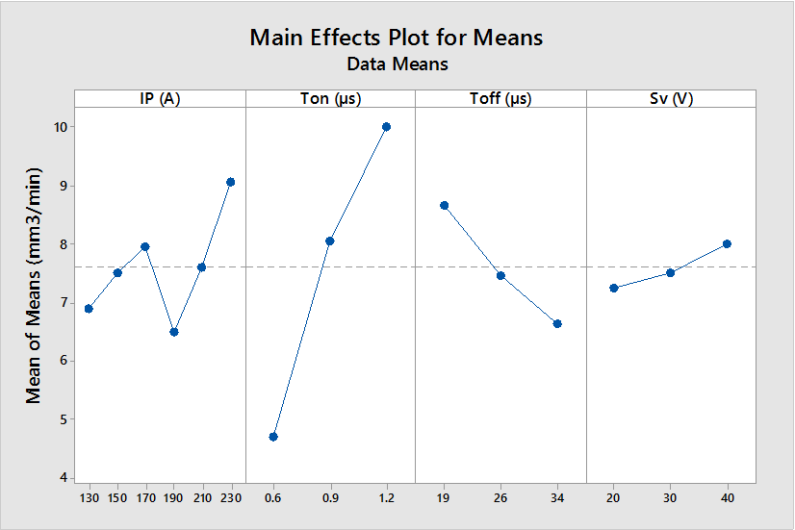

Figure 4.7: Main Effects Plot for MRR Means (Zn Coated Brass Wire)

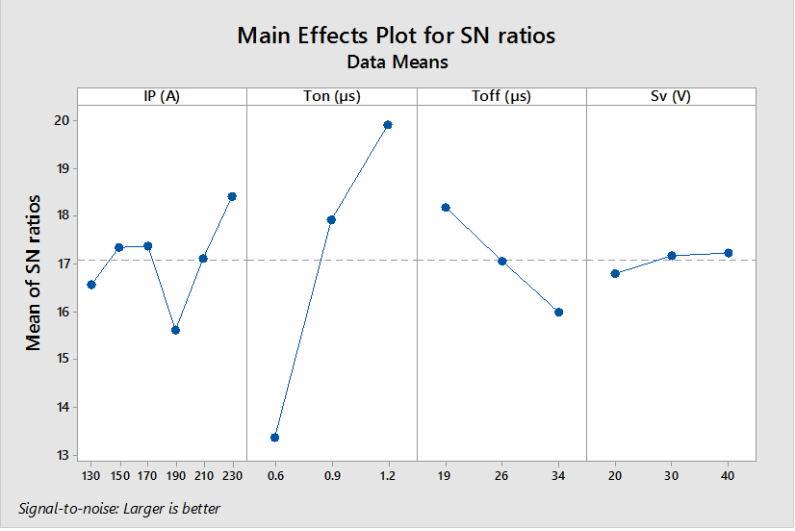

Figure 4.8: Main Effects Plot for SN ratios (Zn Coated Brass Wire)

Table 4.20: Main Effects Plot for MRR SN ratios (Zn coated Brass Wire)

Level	I_P	T_{on}	T_{off}	S_v
1	16.56	13.36	18.53	17.15
2	17.35	18.28	17.05	17.18
3	17.37	19.93	15.99	17.24
4	16.31	-	-	-
5	17.12	-	-	-
6	18.42	-	-	-
Delta	2.11	6.57	2.54	0.09
Rank	3	1	2	4

Table 4.21: Response Table for Means (Zn coated Brass Wire)

Level	I_P	T_{on}	T_{off}	S_v
1	6.906	4.705	8.969	7.543
2	7.525	8.355	7.469	7.525
3	7.966	10.020	6.641	8.012
4	7.079	-	-	-
5	7.609	-	-	-
6	9.076	-	-	-
Delta	2.170	5.315	2.328	0.486
Rank	3	1	2	4

ANOVA Table 4.22 shows the significant effect of parameters. The factor with p-value less than .05 is counted significant due to 95% confidence level taken during analysis. The significant factors for MRR are T_{on} (74.27%) and T_{off} (13.99%), and I_p and S_v is the least significant factor. The R^2 value obtained from the model is .9662 which means 96.62% of the variation is explained by factors considered in this investigation and 3.38% variation is due to error or unexplained by the model. Table 4.23 shows ANOVA calculations for S/N values.

Table 4.22: ANOVA for MRR Mean (Zn coated Brass Wire)

Source	DoF	SS	MS	F- Value	P-value	% Cont.	Significance
I_P	5	9.052	1.8104	2.69	0.130	7.55	Insignificant
T_{ON}	2	88.671	44.3357	65.87	0.000	74.27	Significant
T_{OFF}	2	16.705	8.3527	12.41	0.007	13.99	Significant
S_V	2	0.912	0.4561	0.68	0.543	0.76	Insignificant
Error	6	4.039	0.6731	-	-	-	-
Total	17	119.380	-	-	-	-	-
Model Summary		S		R^2		R^2 (adj)	
		0.820424		96.62%		90.41%	

Table 4.23: ANOVA for MRR S/N ratio (Zn coated Brass Wire)

Source	DoF	SS	MS	F- Value	P-value	% Cont.	Significance
I_P	5	13.12	2.62	2.21	0.182	7.65	Insignificant
T_{ON}	2	135.99	67.99	57.16	0.000	79.34	Significant
T_{OFF}	2	14.49	7.24	6.09	0.036	8.45	Significant
S_V	2	0.68	0.33	0.28	0.763	0.40	Insignificant
Error	6	7.13	1.18	-	-	-	-
Total	17	171.41	-	-	-	-	-
Model Summary		S		R^2		R^2 (adj)	
		1.09069		95.84%		88.20%	

4.2.5 Effect on Surface Roughness with Zinc Coated Brass wire

It is seen from the Fig. 4.3 and Fig. 4.4 that surface roughness increases with the increase in pulse on time. There is a decrease in surface roughness when the value of pulse off time and spark gap set voltage increases. The discharge energy increases by increasing pulse on time and decreasing pulse off time. Lesser pulse off time, more often discharge will occur, results in unstable and more non-uniform MRR. This leads to generate large crater and surface roughness will increase. Increase in spark voltage increases gap between electrodes and results to widening of discharge current and decreases its intensity over small area. Hence, surface roughness decreases.

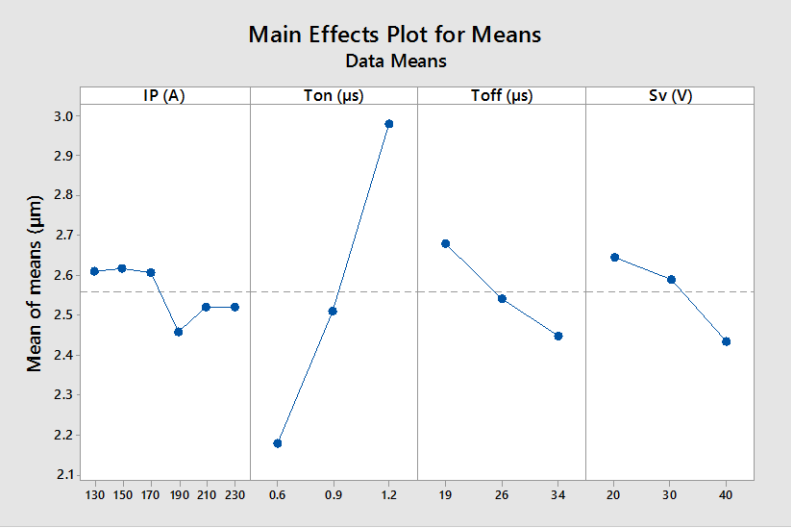

Figure 4.9: Main Effects Plot for SR Means (Zn coated Brass Wire)

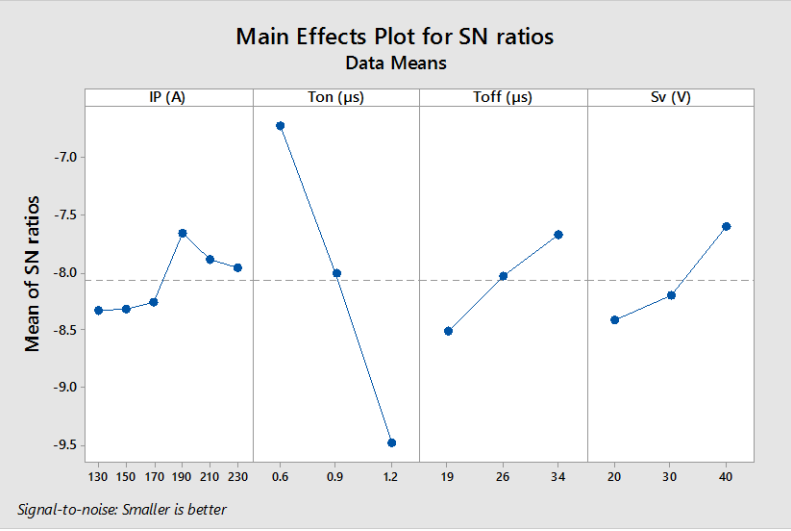

Figure 4.10: Main Effects Plot for SR S/N ratios (Zn coated Brass Wire)

Table 4.24: Response Table for SR S/N Ratios (Zn coated Brass Wire)

Level	I_P	T_{on}	T_{off}	S_v
1	-8.330	-6.721	-8.506	-8.415
2	-8.309	-7.997	-8.022	-8.192
3	-8.254	-9.478	-7.669	-7.590
4	-7.660	-	-	-
5	-7.885	-	-	-
6	-7.954	-	-	-
Delta	0.670	2.757	0.838	0.825
Rank	4	1	2	3

Table 4.25: Response Table for Means (Zn coated Brass Wire)

Level	I_P	T_{on}	T_{off}	S_v
1	2.611	2.079	2.679	2.647
2	2.619	2.511	2.543	2.589
3	2.608	2.980	2.349	2.334
4	2.459	-	-	-
5	2.523	-	-	-
6	2.521	-	-	-
Delta	0.160	0.802	0.230	0.213
Rank	4	1	2	3

The factor with p-value less than .05 is counted significant due to 95% confidence level taken during analysis. ANOVA table 4.26 shows the significant factors for T_{on} (82.76 %), T_{off} (6.8%) and S_v (6.18%) and I_p is the least significant factor. Table 4.27 shows the ANOVA for S/N values.

Table 4.26: ANOVA for Surface Roughness Mean (Zn coated Brass Wire)

Source	DoF	Adj SS	Adj MS	F- Value	P-value	% Cont.	Significance
I_P	5	0.06440	0.012880	2.26	0.175	2.73	Insignificant
T_{ON}	2	1.94669	0.973343	170.49	0.000	82.76	Significant
T_{OFF}	2	0.16112	0.080559	14.11	0.005	6.8	Significant
S_V	2	0.14543	0.072713	12.74	0.007	6.18	Significant
Error	6	0.03425	0.005709	-	-	-	-
Total	17	2.351989	-	-	-	-	-
Model Summary		S		R^2		R^2 (adj)	
		0.0755581		98.54%		95.87%	

Table 4.27: ANOVA for Surface Roughness S/N (Zn coated Brass Wire)

Source	DoF	Adj SS	Adj MS	F- Value	P-value	% Cont.	Significance
I_P	5	1.1232	0.2246	3.12	0.099	3.91	Insignificant
T_{ON}	2	22.8487	11.4244	158.60	0.000	79.59	Significant
T_{OFF}	2	2.1216	1.0608	14.73	0.005	7.39	Significant
S_V	2	2.1831	1.0915	15.15	0.005	7.60	Significant
Error	6	0.4322	0.0720	-	-	-	-
Total	17	28.7088	-	-	-	-	-
Model Summary		S		R^2		R^2 (adj)	
		0.268387		98.49%		95.73%	

4.2.6 Effect on Kerf Width with Zinc Coated Brass Wire

It is observed from the Fig. 4.5 and Fig. 4.6 that kerf width tends to rise by increasing pulse on time and peak current. The graph shows that width of cut decreases with increase in pulse off time. It has been seen that kerf is always greater than the diameter of the wire. The value of kerf width required is less as its large value affects the dimensional accuracy of cutting process. High pulse on time and low pulse off time increases the discharge energy results in high material removal and widen the width of cut. The peak current is least significant in case width of cut and greater the distance between electrodes lesser is the discharge intensity lesser the material erodes lesser will be kerf

Figure 4.11: Main Effects Plot for Kerf Width Means (Zinc Coated Brass Wire)

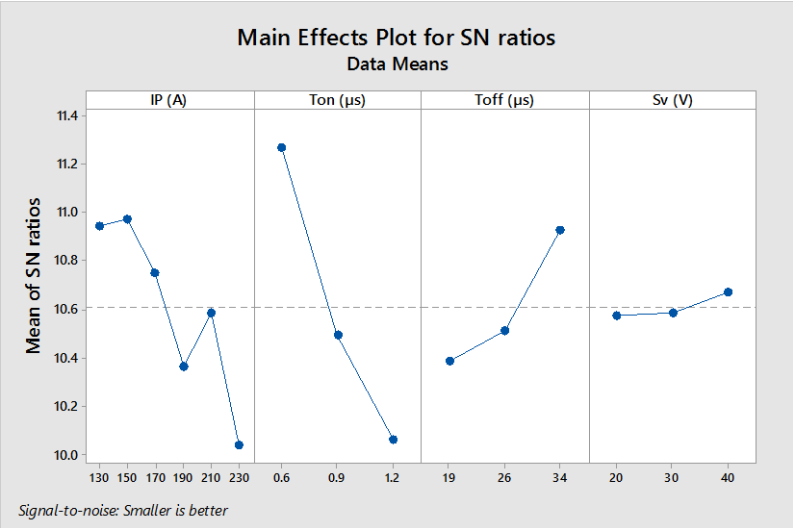

Figure 4.12: Main Effects Plot for Kerf S/N ratios (Zinc Coated Brass Wire)

Table 4.28: Response Table for Kerf Width S/N Ratios (Zn Coated Brass Wire)

Level	I_P	T_{on}	T_{off}	S_v
1	10.94	11.27	10.39	10.57
2	10.97	10.50	10.51	10.59
3	10.75	10.07	10.92	10.67
4	10.36	-	-	-
5	10.59	-	-	-
6	10.04	-	-	-
Delta	0.93	1.20	0.53	0.10
Rank	2	1	3	4

Table 4.29: Response Table for Kerf Means (Zn Coated Brass Wire)

Level	I_P	T_{on}	T_{off}	S_v
1	0.284	0.273	0.303	0.297
2	0.283	0.299	0.299	0.296
3	0.291	0.314	0.284	0.293
4	0.304	-	-	-
5	0.296	-	-	-
6	0.316	-	-	-
Delta	0.033	0.041	0.019	0.004
Rank	2	1	3	4

The factor with p-value less than .05 is counted significant due to 95% confidence level taken during analysis. Table 4.30 shows the significant factors for Kerf Width as T_{on} (53.26%), T_{off} (13.25%) and S_v (11.56%) and I_p is the least significant factor. Table 4.31 shows the ANOVA for S/N values.

Table 4.30: ANOVA for Kerf Width Mean (Zn Coated Brass Wire)

Source	DoF	SS	MS	F- Value	P-value	% Cont.	Significance
I_P	5	0.0022	0.0004	18.35	0.001	29.71	Significant
T_{ON}	2	0.0040	0.0020	82.23	0.000	53.26	Significant
T_{OFF}	2	0.0010	0.0005	22.24	0.002	14.41	Significant
S_V	2	0.00001	0.00002	1.12	0.387	0.72	Insignificant
Error	6	0.0001	0.00002	-	-	-	-
Total	17	0.007513	-	-	-	-	-
Model Summary		S		R^2		R^2 (adj)	
		0.0049315		98.06%		94.50%	

Table 4.31: ANOVA for S/N Kerf Width (Zn Coated Brass Wire)

Source	DoF	SS	MS	F- Value	P-value	% Cont.	Significance
I_P	5	1.938	0.387	10.52	0.006	25.58	Significant
T_{ON}	2	4.444	2.222	60.30	0.000	58.66	Significant
T_{OFF}	2	0.938	0.469	12.73	0.007	12.38	Significant
S_V	2	0.034	0.017	0.47	0.649	0.45	Insignificant
Error	6	0.221	0.036	-	-	-	-
Total	17	7.576	-	-	-	-	-
Model Summary		S		R^2		R^2 (adj)	
		0.191974		91.73%		97.08%	

The main investigation describes various reasons for different behaviour of parameters. The machining characteristics in WEDM usually depend upon the amount of discharge energy generated. The generation of discharge energy generally is a function of pulse duration and intensity of current supplied. Pulse off time has an importance in increasing the stability of machining. It provides the break in current supply duration during which debris is moved away from machining gap by dielectric. Pulse off time also provides time for cooling of workpiece. Its high value results in less surface roughness and high material removal rate and vice versa. Peak current is the intensity of current supplied to form discharge in gap. The investigations show that high current intensity result in high MRR and high surface roughness. The spark gap voltage describes the gap between electrodes and also discharge waiting time depends on it.

4.3 Comparison for machining characteristics

The material removal rate, kerf width and surface roughness for both wires i.e. plain brass wire and zinc coated brass wire are compared in this section. The behavior of all four process parameters is examined and their scatter plot comparison graphs are generated using Minitab 17. It is observed that coated wire has more influence on MRR and SR. Coated wire contains a coating of zinc which has low melting point than core material i.e. brass wire. During current discharge, the zinc coating melts and vaporizes faster than core brass material and some part of zinc get mixed in dielectric. The conductive particles boost breakdown between workpiece and wire and reduces the insulating strength of dielectric fluid which in turn results in early explosion. The faster sparking in gap causes rapid erosion from workpiece. Hence, it improves material removal rate. The uniform distribution of spark due to widening of plasma channel causes uniform erosion resulting in the formation of shallow craters or less surface roughness.

4.3.1 Material Removal rate

The comparison between mean data values for MRR by both wires describes that there is a rise of 24.98% in MRR by zinc coated brass wire as compared to plain brass wire Fig. 4.11 shows the combination of graphs drawn for MRR with respect to four process parameters viz., peak current, pulse on time, pulse off time and spark gap set voltage for both wire. The zinc coated wire shows high MRR in these graphs than plain brass wire. Figure 4.12 shows the comparison graph for mean values of MRR for all the 18 run of experiments.

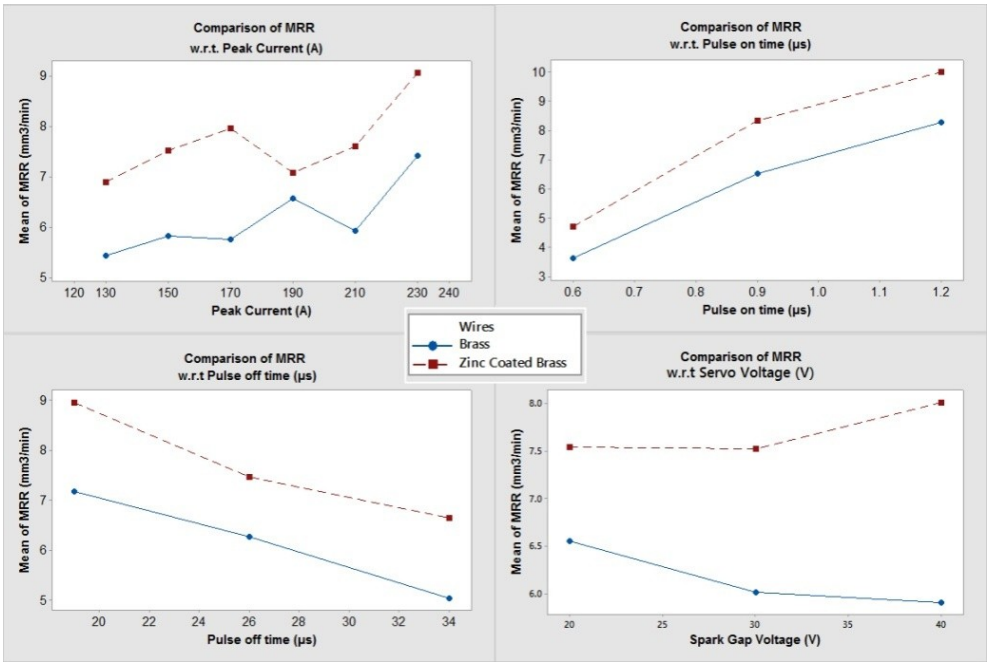

Figure 4.13: Comparison of MRR with both wires

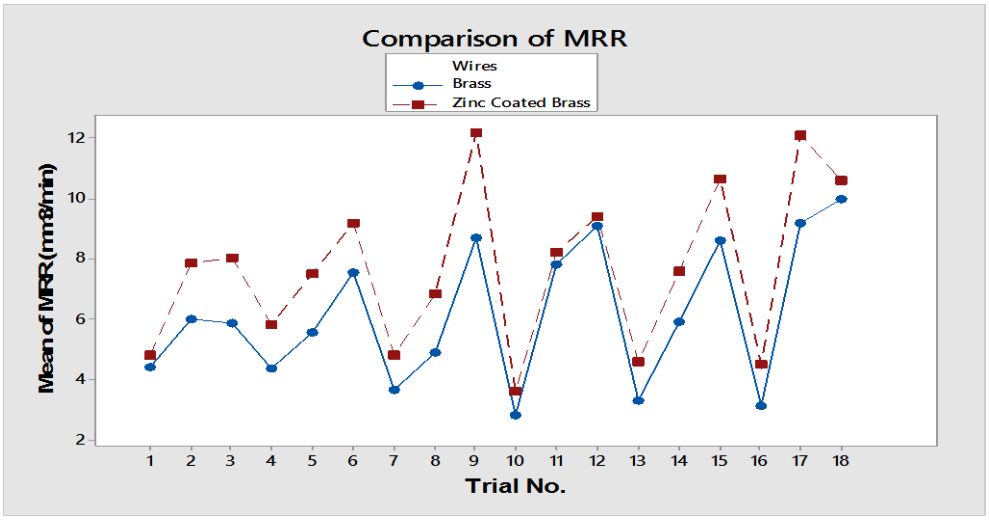

Figure 4.14: Comparison of 18 runs for MRR

4.3.2 Surface Roughness

Surface roughness is the measure of surface texture, smooth or rough. Surface texture in WEDM depends upon number of factors. It is observed that smooth surface texture is obtained by uniform and slow cutting rate. Figure 4.13 shows combination of graphs which compares the surface roughness between brass wire and zinc coated brass wire for each process parameter. The calculated results reveal that there is overall decrease of 7.54% in surface roughness when machining is done with coated wire as compared to plain brass wire.

Figure 4.14 shows the overall comparison for each trial with both wires for surface roughness.

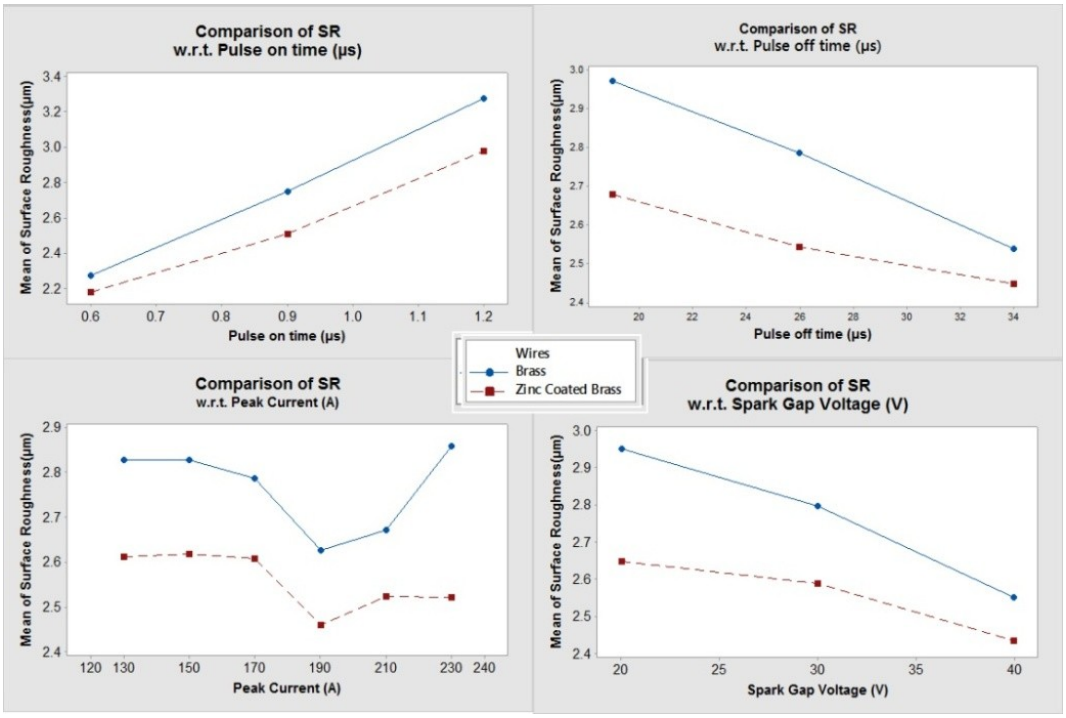

Figure 4.15: Comparison of SR with both wires

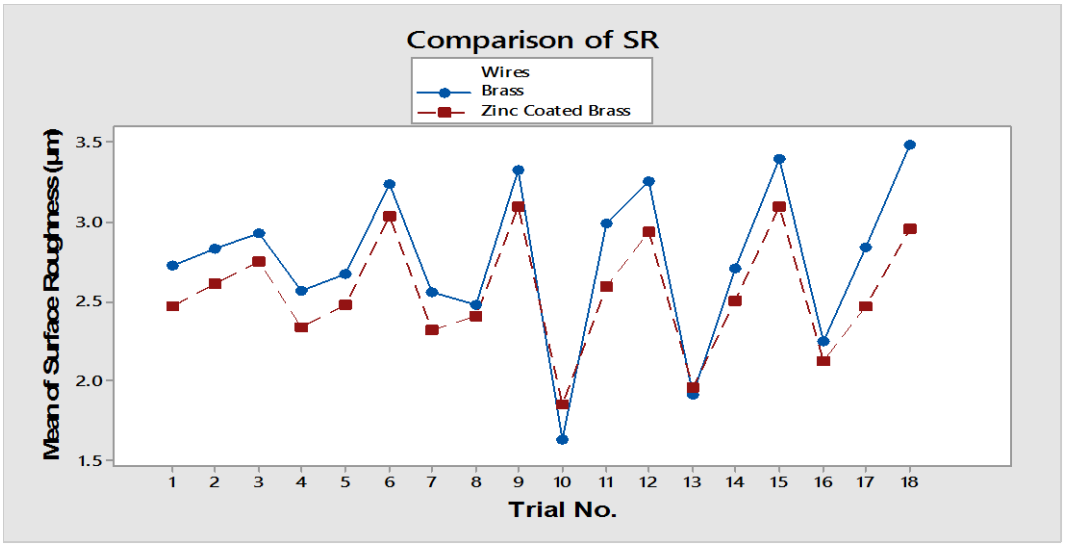

Figure 4.16: Comparison of 18 runs for SR

4.3.3 Kerf Width

Kerf width is the width of cut generated by the wire in the workpiece during cutting operation. This section compares the kerf width generated for both wire at same levels of process parameters. Figure 4.15 shows the comparison graphs for kerf width with respect to

different parameters. The calculated results reveal that there is overall increase of 5.10% in kerf width when machining is done with coated wire as compared to plain brass wire. Figure 4.16 shows the overall comparison for each trial with both wires for kerf width.

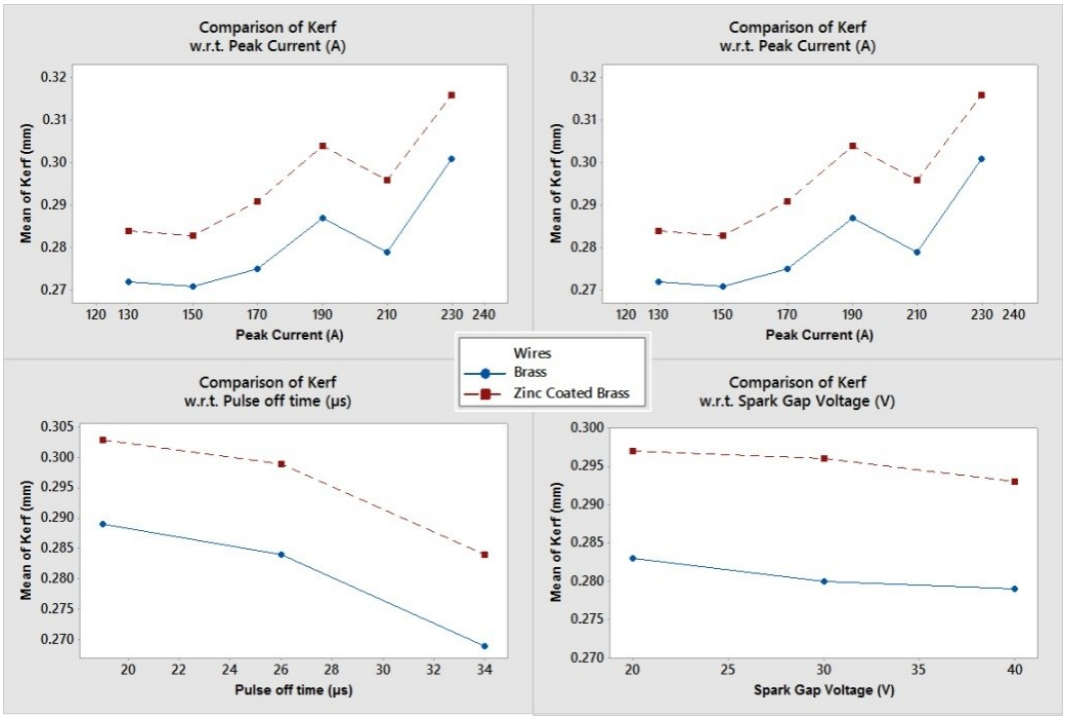

Figure 4.17: Comparison of Kerf width with both wires

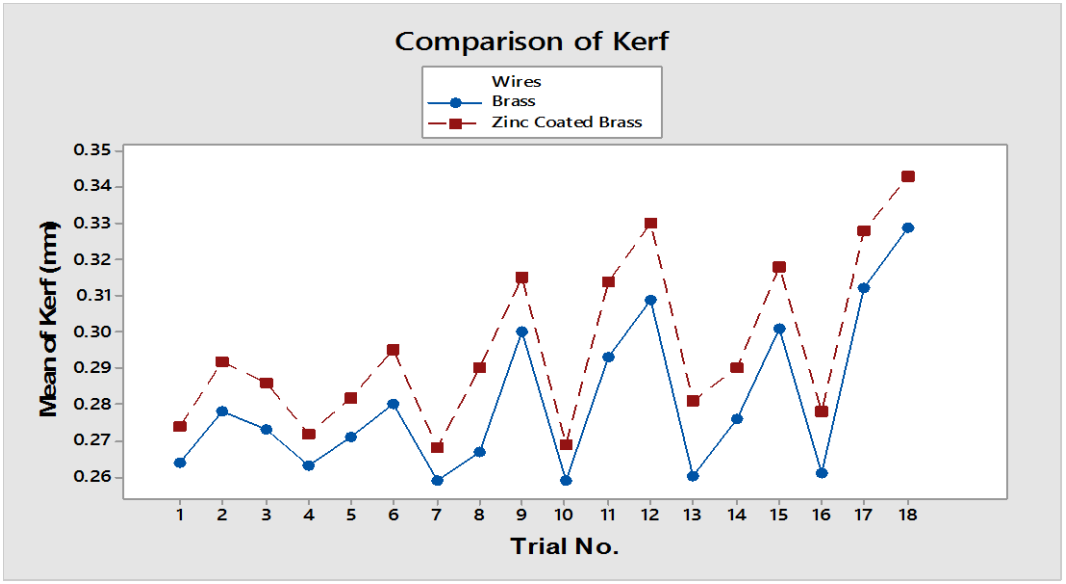

Figure 4.18: Comparison of 18 runs for kerf width

Chapter 5

Optimization & Confirmation Experiments

5.1 Optimization and Prediction

The Optimization is a method to find the optimum levels of parameters for desired machining performance. There are two types of optimization techniques, single objective optimization and multi-objective optimization. Optimization can be done by using various techniques like RSM, Grey Relational Analysis, Taguchi's Method etc. In this research work, single objective optimization is done using Taguchi's S/N ratio delta statics and multi objective optimization is done using multi response signal to noise ratio (MRSN) technique. Predicted values from the optimum selected levels are calculated for machining performances to get the idea of output values.

5.1.1 Single Objective Optimization

The purpose of single objective optimization is to find optimum parameters that are beneficial for single machining parameter. For example, if the requirement is to get high MRR, levels of parameters can be chosen so that these levels of parameters give high MRR and it has no relation with the outcome of surface roughness or any other machining performances. In this section, objectives of optimization are high MRR, low surface roughness and least kerf width.

i. Selection of optimal parameters for MRR (plain brass wire):

The optimum parameters are selected by selecting levels having high value of S/N ratio for each parameter from response tables. The optimal parameters form high MRR with plain brass wire are shown in table 5.1. The MRR values at optimal levels are taken from section 4.2.1 and Table 4.9.

Table 5.1: Optimal Levels for MRR (Brass Wire)

Factor	I_P (A)	T_{ON} (µs)	T_{OFF} (µs)	S_V (V)
Actual Value	230	1.2	19	20
Optimum Level	6	3	1	1

Prediction for MRR with optimal parameters

The high value for MRR can be predicted from following equation using optimum levels of parameters. Eq. (5.1) & (5.2) describes the calculation for MRR at optimal levels.

$$\propto_{MRR} = I_{p\ 6} + T_{on\ 3} + T_{off\ 1} - 2 \times \mu_{MRR} \quad (5.1)$$

Where; $\propto_{MRR}$=Predicted Average

μ_{MRR}= overall mean for MRR with plain brass wire

$$\propto_{MRR} = 8.30 + 7.17 + 6.55 - 2 \times (6.15) \quad (5.2)$$

$$\propto_{MRR} = 10.6\ mm^3/min$$

ii. Selection of optimal parameters for Surface Roughness (Plain Brass wire):

The optimum parameters are selected by selecting levels having high value of S/N ratio for each parameter from response tables. The optimal parameters form low SR with plain brass wire are shown in table 5.2.

Table 5.2: Optimal Levels for Surface Roughness (Brass Wire)

Factor	I_P (A)	T_{ON} (µs)	T_{OFF} (µs)	S_V (V)
Actual Value	190	0.6	34	40
Optimum Level	4	1	3	3

Prediction for Surface Roughness with optimal parameters

The high value for SR can be predicted from following equation using optimum levels of parameters. The surface roughness values at optimal levels are taken from section 4.2.2 and Table 4.13. Eq. (5.3) & (5.4) describes the calculation for surface roughness at optimal levels.

$$\propto_{SR} = T_{ON\ 1} + T_{OFF\ 3} + S_{V\ 3} - 2 \times \mu_{SR} \quad (5.3)$$

Where,$\propto_{SR}$= Predicted Average

μ_{SR}= overall mean for surface roughness with plain brass wire

$$\propto_{SR} = 2.174 + 2.440 + 2.550 - 2 \times (2.766) \quad (5.4)$$

$$\propto_{SR} = 1.632\ \mu m$$

iii. Selection of optimal parameters for Kerf (plain brass wire):

The optimum parameters are selected by selecting levels having high value of S/N ratio for each parameter from response tables. The optimal parameters for low Kerf Width with plain brass wire are shown in table 5.3. The kerf values at optimal levels are taken from section 4.2.3 and Table 4.17.

Table 5.3: Optimal Levels for Kerf (Brass Wire)

Factor	I_P (A)	T_{ON} (µs)	T_{OFF} (µs)	S_V (V)
Actual Value	150	0.6	34	40
Optimum Level	2	1	3	3

Prediction for Kerf Width with optimal parameters

The high value for Kerf can be predicted from following equation using optimum levels of parameters. Eq. (5.5) & (5.6) describes the calculation for kerf width at optimal levels.

$$\propto_{Kerf} = I_{P\,2} + T_{ON\,1} + T_{OFF\,3} - 2 \times \mu_{Kerf} \quad (5.5)$$

Where; $\propto_{Kerf}$ = Predicted Average

μ_{Kerf} = overall mean for kerf with plain brass wire

$$\propto_{Kerf} = 0.271 + 0.261 + 0.269 - 2 \times (0.280) \quad (5.6)$$

$$\propto_{Kerf} = .249\ mm$$

iv. Selection of optimal parameters for MRR (zinc coated brass wire) :

The optimum parameters are selected by selecting levels having high value of S/N ratio for each parameter from response tables. The optimal levels of parameters for high MRR with zinc coated brass wire are shown in table 5.4. The MRR values at optimal levels are taken from section 4.2.4 and Table 4.21.

Table 5.4: Optimal Levels for MRR (Zn coated Brass Wire)

Factor	I_P (A)	T_{ON} (µs)	T_{OFF} (µs)	S_V (V)
Actual Value	230	1.2	19	40
Optimum Level	6	3	1	3

Prediction for MRR with optimal parameters

The high value for MRR can be predicted from following equation using optimum levels of parameters. . Eq. (5.7) & (5.8) describe the calculation for MRR at optimal levels.

$$\alpha'_{\mathrm{MRR}} = T_{ON\,3} + T_{OFF\,1} - \mu'_{\mathrm{MRR}} \quad (5.7)$$

Where, α'_{MRR} = Predicted Average

μ'_{MRR} = overall mean for MRR with zinc coated brass wire

$$\alpha'_{\mathrm{MRR}} = 10.020 + 8.969 - (7.693) \quad (5.8)$$

$$\alpha'_{\mathrm{MRR}} = 11.269\ mm^3/min$$

v. Selection of optimal parameters for SR (zinc coated brass wire):

The optimum parameters are selected by selecting levels having high value of S/N ratio for each parameter from response tables. The optimal levels of parameters for low surface roughness with zinc coated brass wire are shown in table 5.5. The surface roughness values at optimal levels are taken from section 4.2.5 and Table 4.25.

Table 5.5: Optimal Levels for Surface Roughness (Zn coated Brass Wire)

Factor	I_P (A)	T_{ON} (µs)	T_{OFF} (µs)	S_V (V)
Actual Value	190	0.6	34	40
Optimum Level	4	1	3	3

Prediction for SR with optimal parameters

The low value for SR can be predicted from following equation using optimum levels of parameters. Eq. (5.9) & (5.10) describe the calculation for MRR at optimal levels.

$$\alpha'_{SR} = T_{ON\,1} + T_{OFF\,3} + S_{V\,3} - 2 \times \mu'_{SR} \quad (5.9)$$

Where; α'_{SR} = Predicted Average

μ'_{SR} = overall mean for surface roughness with zinc coated brass wire

$$\alpha'_{SR} = 2.079 + 2.349 + 2.334 - 2 \times 2.556 \quad (5.10)$$

$$\alpha'_{SR} = 1.65\ \mu m$$

vi. Selection of optimal parameters for Kerf (zinc coated brass wire):

The optimum parameters are selected by selecting levels having high value of S/N ratio for each parameter from response tables. The optimal parameters for low Kerf Width with zinc coated brass wire are shown in Table 5.6. The surface roughness values at optimal levels are taken from section 4.2.6 and Table 4.29.

Table 5.6: Optimal Levels for Kerf (Zn coated Brass Wire)

Factor	I_P (A)	T_{ON} (µs)	T_{OFF} (µs)	S_V (V)
Actual Value	150	0.6	34	40
Optimum Level	2	1	3	3

Prediction for Kerf Width with optimal parameters

The low value for Kerf Width can be predicted from following equation using optimum levels of parameters. Eq. (5.11) & (5.12) describe the calculation for kerf at optimal levels.

$$\alpha'_{kerf} = I_{P\,2} + T_{ON\,1} + T_{OFF\,3} - 2 \times \mu_{Kerf} \quad (5.11)$$

Where; α'_{Kerf} = Predicted Average

μ'_{Kerf} = overall mean for kerf with zinc coated brass wire

$$\alpha'_{\text{kerf}} = 0.283 + 0.273 + 0.284 - 2 \times 0.295 \quad (5.12)$$

$$\alpha'_{\text{kerf}} = .26\ mm$$

5.1.2 Multi objective optimization

Multi-objective optimization is method to find out optimum levels of parameters which give desired results for two or more than two machining performance parameters. These levels affect the results of more than one response. In this section, multi-objective optimization is done on two machining performances. As material removal rate and surface roughness are the most desired outputs of any manufacturing process, both have taken for the optimization. To make the optimization economical, equal importance is given to both machining parameters. Multi objective optimization is done using multi response signal noise ratio (MRSN). MRSN is a method designed by Taguchi to optimize multi response characteristics. Since, most of the output response characteristics have different measurement unit and different group in S/N ratio calculations, so it is not possible to perform analysis. MRSN method includes following steps to perform multi objective characterization [Gaitonde et al., 2006].

Step 1- Calculate the loss function (L_{ij}).

For smaller the better, Eq. (5.13)

$$L_{ij} = \frac{1}{n}\sum_{k=1}^{n} y_{ijk}^2 \quad (5.13)$$

For larger is better, Eq. (5.14)

$$L_{ij} = \frac{1}{n}\sum_{k=1}^{n} \frac{1}{y_{ijk}^2} \quad (5.14)$$

where, n is the no. of repeated experiments. (L_{ij}) is loss function of the i^{th} performance characteristic in the j^{th} experiment. Y_{ijk} is the experimental value of the i^{th} performance characterizes in the j^{th} experiment at the k^{th} test.

Step 2- Calculate normalized quality loss i.e. N_{ij} as described in Eq. (5.15)

$$N_{ij} = \frac{L_{ij}}{L_i^*} \quad (5.15)$$

Where; $L_i^* = \frac{1}{n}\sum_{i=1}^{n} L_{ij}$

Step 3- Eq. (5.16) describes the total loss function ($TL_{j)}$. Weights are applied according to the priority of each normalized loss function. This method defines the importance of every response characteristic.

$$TL_j = \sum_{i=1}^{p} W_i N_{ij} \quad (5.16)$$

Where, *Wi* is the weighting factor, *p* is the total number of quality characteristics.

Step 4- The overall S/N ratio is calculated in this step to perform multi-objective optimization. This overall S/N ratio is known as multiple response S/N ratio (MRSN). The calculation method multiple response S/N ratio (MRSN) is described in Eq. (5.17):

$$MRSN = -10 \log(TL_j) \quad (5.17)$$

The results obtained by using steps 1-4 are shown in Table 5.7 and 5.8 for plain brass wire and for zinc coated brass wire respectively.

Table 5.7: MRSN values Plain Brass wire

Run	L_{ij}		$N_{ij}=L_{ij}/L_i^*$		$W_i N_{ij}$		TL_j	MRSN (db)
	MRR	SR	MRR	SR	MRR W=5	SR W=5		
1	0.051	7.436	1.224	0.935	6.118	4.675	10.792	-10.331
2	0.028	8.001	0.669	1.006	3.344	5.030	8.374	-9.229
3	0.029	8.625	0.689	1.084	3.446	5.422	8.869	-9.479
4	0.053	6.605	1.263	0.830	6.316	4.152	10.468	-10.199
5	0.032	7.133	0.776	0.897	3.881	4.484	8.365	-9.225
6	0.018	10.515	0.420	1.322	2.101	6.611	8.712	-9.401
7	0.073	6.542	1.759	0.823	8.797	4.113	12.910	-11.109
8	0.042	6.134	1.000	0.771	4.999	3.856	8.855	-9.472
9	0.013	11.106	0.316	1.396	1.579	6.982	8.561	-9.325
10	0.127	2.658	3.045	0.334	15.223	1.671	16.894	-12.277
11	0.016	8.912	0.393	1.121	1.963	5.603	7.566	-8.789
12	0.012	10.644	0.290	1.338	1.448	6.692	8.140	-9.106
13	0.092	3.639	2.200	0.458	10.998	2.288	13.286	-11.234
14	0.029	8.324	0.686	1.047	3.430	5.233	8.663	-9.377
15	0.014	11.590	0.324	1.457	1.619	7.287	8.906	-9.497
16	0.101	5.075	2.422	0.638	12.110	3.190	15.301	-11.847
17	0.012	8.037	0.285	1.011	1.423	5.053	6.476	-8.113
18	0.010	12.182	0.241	1.532	1.205	7.658	8.863	-9.476

L_i^* (MRR) =0.042, L_i^* (SR) =7.953

Table 5.8: MRSN values Zinc coated brass wire

Run	L_{ij}		$N_{ij}=L_{ij}/L_i^*$		$W_i N_{ij}$		TL_j	MRSN (db)
	MRR	SR	MRR	SR	MRR W=5	SR W=5		
1	0.043	6.115	1.735	0.917	8.673	4.584	13.257	-11.224
2	0.016	6.821	0.655	1.023	3.276	5.114	8.390	-9.238
3	0.015	7.563	0.626	1.134	3.131	5.669	8.800	-9.445
4	0.029	5.488	1.185	0.823	5.926	4.114	10.041	-10.018
5	0.018	6.142	0.713	0.921	3.564	4.604	8.169	-9.122
6	0.012	9.227	0.487	1.383	2.433	6.917	9.350	-9.708
7	0.043	5.362	1.750	0.804	8.751	4.020	12.771	-11.062
8	0.021	5.820	0.858	0.873	4.291	4.363	8.654	-9.372
9	0.007	9.595	0.271	1.439	1.356	7.193	8.549	-9.319
10	0.076	3.435	3.071	0.515	15.354	2.575	17.929	-12.536
11	0.015	6.712	0.601	1.006	3.007	5.032	8.038	-9.052
12	0.011	8.615	0.456	1.292	2.282	6.458	8.740	-9.415
13	0.048	3.833	1.925	0.575	9.626	2.874	12.499	-10.969
14	0.017	6.288	0.702	0.943	3.508	4.714	8.222	-9.150
15	0.009	9.626	0.356	1.443	1.781	7.216	8.997	-9.541
16	0.049	4.550	1.973	0.682	9.863	3.411	13.274	-11.230
17	0.007	6.103	0.277	0.915	1.384	4.575	5.959	-7.751
18	0.009	8.762	0.359	1.314	1.795	6.569	8.364	-9.224

L_i^* (MRR) =0.025, L_i^* (SR) =6.670

According to delta statistics described in Table 5.9 & 5.10, ranks are assigned to the factors as per their significance value. The delta value is obtained by subtracting smaller value from the larger value for each factor and ranks are assigned accordingly. Highest delta value got the highest rank. The optimum parameters are selected by selecting levels having high value of S/N ratio for each parameter from response tables.

Table 5.9: Response values for MRSN Ratio (Plain Brass wire)

LEVELS	I_P	T_{on}	T_{off}	S_V
1	-9.68	-11.17	-9.38	-9.75
2	-9.61	-9.03	-9.90	-9.89
3	-9.97	-9.38	-10.31	-9.94
4	-10.06			
5	-10.04			
6	-9.81			
DELTA	0.45	2.13	0.93	0.20
Rank	3	1	2	4

Table 5.10: Response values for MRSN Ratio (Zinc Coated brass wire)

LEVELS	IP	Ton	Toff	SV
1	-9.97	-11.17	-9.48	-9.90
2	-9.62	-8.95	-9.84	-9.80
3	-9.92	-9.44	-10.24	-9.86
4	-10.33			
5	-9.89			
6	-9.40			
DELTA	0.93	2.22	0.76	0.10
RANK	2	1	3	4

The factor with p-value less than .05 is counted significant due to 95% confidence level taken during analysis. ANOVA Table 5.11 shows the percentage contribution of factors variation in case for MRSN plain brass wire as T_{on} (76.77%), T_{off} (12.81%), I_p (2.63%) and S_v (0.59%) is the least significant factor. ANOVA Table 5.12 shows the contribution of factors for variation for MRSN in case of zinc coated brass wire as T_{on} (76.02%), T_{off} (7.93%), I_p (7.09%) and S_v (0.13%) is the least significant factor.

Table 5.11: ANOVA for MRSN values (Plain brass wire)

Source	DoF	SS	MS	F- Value	P-value	% Contribution	Significance
IP	5	0.5397	0.1079	0.45	0.804	2.63	Insignificant
Ton	2	15.7070	7.8535	32.38	0.001	76.77	Significant
Toff	2	2.6242	1.3120	5.41	0.045	12.81	Significant
SV	2	0.1229	0.0614	0.25	0.784	0.59	Insignificant
Error	6	1.4550	0.2425	-	-	-	-
Total	17	20.4488	-	-	-	-	-

Table 5.12: ANOVA for MRSN values (Zinc coated brass wire)

Source	DoF	SS	MS	F- Value	P-value	% Contribution	Significance
IP	5	1.5309	0.3061	0.97	0.503	7.09	Insignificant
Ton	2	16.3901	8.1950	25.94	0.001	76.02	Significant
Toff	2	1.7169	0.8584	2.72	0.144	7.93	Insignificant
SV	2	0.0307	0.0153	0.05	0.953	0.13	Insignificant
Error	6	1.8956	0.3159	-	-	-	-
Total	17	21.5642	-	-	-	-	-

i. Selection of optimal parameters for MRSN (Plain brass wire) :

The optimum parameters are selected by selecting levels having high value of S/N ratio for each parameter from response Table 5.9. The optimal levels of parameters for high MRSN with plain brass wire are shown in Table 5.13.

Table 5.13: Optimum levels for MRSN (Plain Brass wire)

Factor	I_P (A)	T_{ON} (µs)	T_{OFF} (µs)	S_V (V)
Actual Value	150	0.9	19	20
Optimum Level	2	2	1	1

Prediction for MRSN with optimal parameters

The high value for MRSN can be predicted from following equation using optimum levels of parameters. The MRSN values at optimal levels are taken from Table 5.9. Eq. (5.18) & (5.19) describe the calculation for MRSN at optimal levels.

$$\alpha_{MRR} = T_{ON\,2} + T_{OFF\,1} - \mu'_{MRSN} \quad (5.18)$$

Where,

α_{MRSN} = Predicted Average

μ_{MRSN} = overall mean for MRSN with plain brass wire

$$\alpha_{MRR} = (-9.03) + (-9.38) - (-9.861) \quad (5.19)$$

$$\alpha_{MRSN} = -8.54 \text{ db}$$

ii. Selection of optimal parameters for MRSN (zinc coated brass wire) :

The optimum parameters are selected by selecting levels having high value of S/N ratio for each parameter from response Table 5.10. The optimal levels of parameters for high MRSN with zinc coated brass wire are shown in Table 5.14.

Table 5.14: Optimum levels for MRSN (Zinc coated brass wire)

Factor	I_P (A)	T_{ON} (µs)	T_{OFF} (µs)	S_V (V)
Actual Value	230	0.9	19	30
Optimum Level	6	2	1	2

Prediction for MRSN with optimal parameters

The high value for MRSN can be predicted from following equation using optimum levels of parameters. The MRSN values at optimal levels are taken from Table 5.10. Eq. (5.20) & (5.21) describe the calculation for MRSN at optimal levels.

$$\alpha'_{\text{MRSN}} = T_{ON\,2} \tag{5.20}$$

Where,

α'_{MRSN} = Predicted Average

μ'_{MRSN} = overall mean for MRSN with zinc coated brass wire

$$\alpha'_{\text{MRSN}} = (-8.95) - 0 \times (-9.854) \tag{5.21}$$

$$\alpha'_{\text{MRSN}} = -8.95 \text{ db}$$

5.2 Confirmation Experiments

Confirmation experiment is the concluding part of machining process. Machining is performed on WEDM using optimum levels of parameters to examine the results. Confirmatory experiments are done to relate the results with predicted values and find the difference between predicted and experimented value. Following tables shows the results of confirmatory experiments. The value of error is also examined for experimental value with respect to predicted value.

5.2.1 Confirmatory results for plain brass wire

The confirmation experiment for high MRR with brass wire shows that MRR increases by 11.41%. The Confirmatory experiment for lower surface roughness shows very significant improvement for optimal parameters. However, there is a difference between the predicted value and experimental value but surface roughness in confirmation experiments decreases by 15.78 %. The Experiment shows that the kerf width has increased than predicted value with an error of 7.08%. The values for MRR, SR and kerf are shown in Table 5.15.

Table 5.15: Confirmatory Experiment Values for Plain Brass Wire

S. No.	Response	Predicted value*	Experimental value	Change
1	Material Removal Rate (mm^3/min)	10.6	11.41	3.68 %
2	Surface Roughness (μm)	1.54	1.33	15.78 %
3	Kerf Width (mm)	.249	.268	7.08 %

*Predicted Value- Calculated in Section 5.1.1 (i, ii, iii)

5.2.2 Confirmatory results for Zinc coated brass wire

The confirmatory experiment shows an increase of 21.19% from predicted value of MRR. It is a significant increase. The high value of MRR is always required for rapid cutting rate. The surface roughness is decreased by 10% when confirmatory experiments were done using optimal levels of parameters for low surface roughness by zinc coated brass wire. The Experiment shows that the kerf width has increased than predicted value with an error of 8.45%. The values for MRR, SR and kerf are shown in Table 5.16.

Table 5.16: Confirmatory Experiment Values for Zinc Coated Brass Wire

S. No.	Response	Predicted value*	Experimental value	Change
1	Material Removal Rate (mm^3/min)	11.269	14.30	21.19 %
2	Surface Roughness (μm)	1.65	1.50	10 %
3	Kerf Width (mm)	.260	.284	8.45 %

* Predicted Value- Calculated in Section 5.1.1 (iv, v, vi)

5.2.3 Confirmatory Results MRSN Plain Brass wire

Table 5.17 shows the data obtained by using Eq. (5.13) – Eq. (5.17) to find MRSN value for confirmatory experiments. Table 5.18 shows the values for predicted values for MRSN and values obtained by experiments performed at optimum levels of parameters to achieve maximum MRR and less surface roughness. The error obtained from predicted MRSN value to experimental value is 13.86%.

Table 5.17 Calculation of MRSN value for confirmatory experiment

Experimental Values		L_{ij}		$N_{ij}=L_{ij}/L_i^*$		$W_i N_{ij}$		TL_j	MRSN (db)
MRR	SR	MRR	SR	MRR	SR	MRR W=5	SR W=5		
6.97	2.41	0.021	5.808	0.493	0.730	2.465	3.651	6.117	-7.86

L_i^* (MRR)=0.042, L_i^* (SR)=7.953

Table 5.18: Error obtained for MRSN Plain brass wire

S. No.	Response	Predicted value	Experimental value	Error %
1	Material Removal Rate (mm^3/min)	-	6.97	-
2	Surface Roughness (μm)	-	2.40	-
3	MRSN (db)	-8.95	-7.86	13.86 %

5.2.4 Confirmatory Results MRSN Zinc coated Brass wire

Table 5.19 describes the data obtained by applying Eq. (5.13) – Eq. (5.17) to find MRSN value for confirmatory experiments. Table 5.20 shows the values for predicted values for MRSN and values obtained by experiments performed at optimum levels of parameters to achieve maximum MRR and less surface roughness. The error obtained from predicted MRSN value to experimental value is 7.15%.

Table 5.19 Calculation of MRSN value for confirmatory experiment

Experimental Values		L_{ij}		$N_{ij}=L_{ij}/L_i^*$		$W_i N_{ij}$		TL_j	MRSN (db)
MRR	SR	MRR	SR	MRR	SR	MRR W=5	SR W=5		
9.45	2.31	0.011	5.336	0.453	0.800	2.263	4.000	6.263	-7.968

L_i^* (MRR)=0.025, L_i^* (SR)=6.670

Table 5.20: Error obtained for MRSN Zinc coated brass wire

S. No.	Response	Predicted value	Experimental value	Error %
1	Material Removal Rate (mm^3/min)	-	9.45	-
2	Surface Roughness (μm)	-	2.31	-
3	MRSN (db)	-8.54	-7.97	7.15 %

Chapter 6

Surface Characterization

6.1 Surface Topography

The surface obtained by EDM is created by a sequence of distinct precisely controlled spark produced between electrodes, which create craters in the exposed surface. This process is suitable for machining any conducting materials regardless of its hardness, brittleness, strength, or toughness of the workpiece and the tool doesn't have to be harder than the workpiece as there is no mechanical contact during machining. A series of electrical discharges cause explosion due to which sudden pressure is generated and molten material is removed. Due to rapid local heating and cooling, multi layered surface is created on the workpiece. This consists of three layers namely: recast or white layer on the top of the work surface, the Heat Affected Zone (HAZ), and the transformed layer where a change in grain structure from the base structure is apparent as shown in figure 6.1. The formation of these layers depends on the process conditions and workpiece properties like chemical composition and thermal conductivity [Ramasawmy et al., 2005].

The molten material produced during the spark is partly flushed away by the dielectric, and the rest re-solidifies that forms the white layer at the top. It alters metallurgical structure after going through the extremely high energy thermal process accompanied by dielectric cooling process. This layer usually differs significantly from the base material and it is generally very fine grained and hard. It may be alloyed with carbon released from the cracked dielectric or with material transferred from the tool. It is observed that the white layer contains pock marks, pores, micro-cracks which are unfavorable for the functional behavior of the components.

The next layer is the Heat Affected Zone (HAZ). It is the base material that has been heated and structurally altered, due to elevation to the austenitising temperature range. This zone may contain re-harden brittle, untempered martensite that is formed during rapid cooling. This microstructure stores considerable strain energy that decomposes with heat and results in crack formation. Below this layer usually a transformed layer exists where the temperature attained is not as high, and the hardness is therefore, less than the original material. The relative depth of these layers, and even their presence, depends on what type of

EDM method used. The quick heating and cooling effect in EDM persuade a high-temperature gradient within the heat affected area and therefore cause a significant stress within the machined surface.

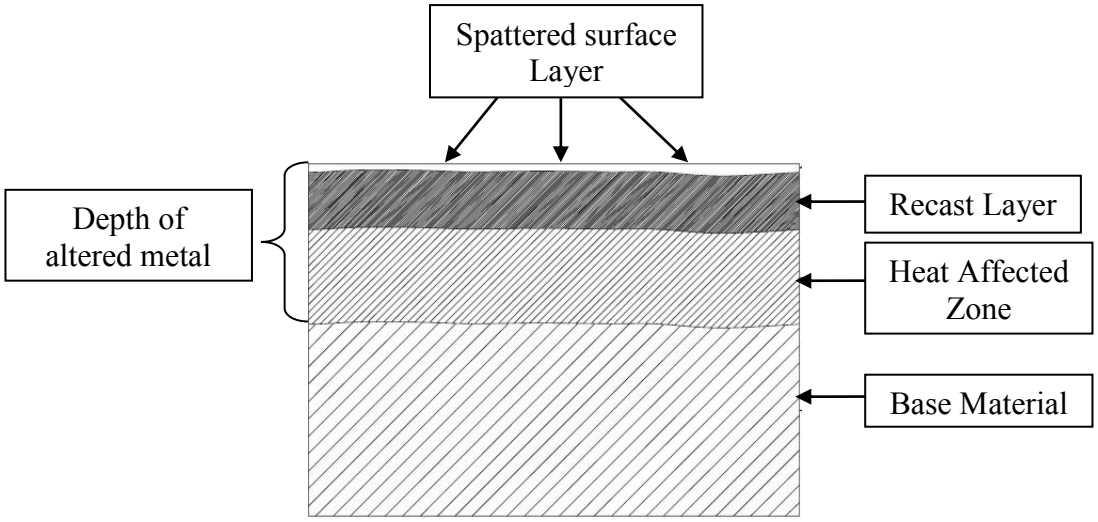

Figure 6.1 Metal zones altered by WEDM [Sommer and Sommer, 2005]

The formation of crack is due to the differential of high contraction stresses induced during the EDM process. When the induced stress exceeds the material's ultimate tensile strength there is formation of crack in the EDMed surface [Lee et al., 1992]. To enhance the life of the EDMed product, the recast layer is normally removed as this layer plays a critical role especially for applications in which the part is subjected to cylindrical stress or fluctuating loads. It is usually observed that the cracks are initiated from the top surface and propagate in the white layer and terminate at the white layer and HAZ interface, and rarely do they cross the HAZ. It is well known fact that for characterization of quality of EDMed component surface plays a vital role. The component having a good surface improves the fatigue strength, wear resistance and corrosion resistance of the surface [Tai and Lu (2009)]. Consequently, the white layer must be removed by hand polishing, etching to improve the properties and make the component functional. Usually with abrasive grains such as silicon carbide, alumina, or diamond, are used to polish the surface in the presence of a lubricant, to achieve the mirror-like finish. The polishing must be done appropriately just to remove the white layer, which causes damage to the component, but excessive polishing may lead to removal of excess material and loose precision.

In this study, we have used SEM and EDX to examine the microstructure and composition of the layers of the machined sample.

6.1.1 Scanning Electron Microscopy (SEM)

The influence of Wire EDM parameters and different wires on surface formed during machining can be observed from the SEM micrographs. To study the recast layer on the machined surface, the sample was simply rinsed in acetone for a short period to remove unnecessary impurities like dust particle, rust etc.. To study the surface and cracks formed due to heat affected zone, the sample is polished with EMBRI paper (Grade 100, 1200, 1500, 2000, 3000) for polishing purpose and then sample is immersed in Nital Acid (3 ml HNO_3, 47 ml Alcohol) which act as etchant for D2 steel to reveal microstructure. The SEM images for recast layer are taken for two samples; one machined with plain brass wire and other with zinc coated wire, to compare the difference obtained in formation of recast layer with different wires. The figure 6.2 shows the recast layer formed on surface at parameters; T_{ON}=1.2 µs, T_{OFF}=26 µs, I_P=230 A and S_V=20 V. The mean thickness obtained by these set of levels of parameters is 7.814 µm.

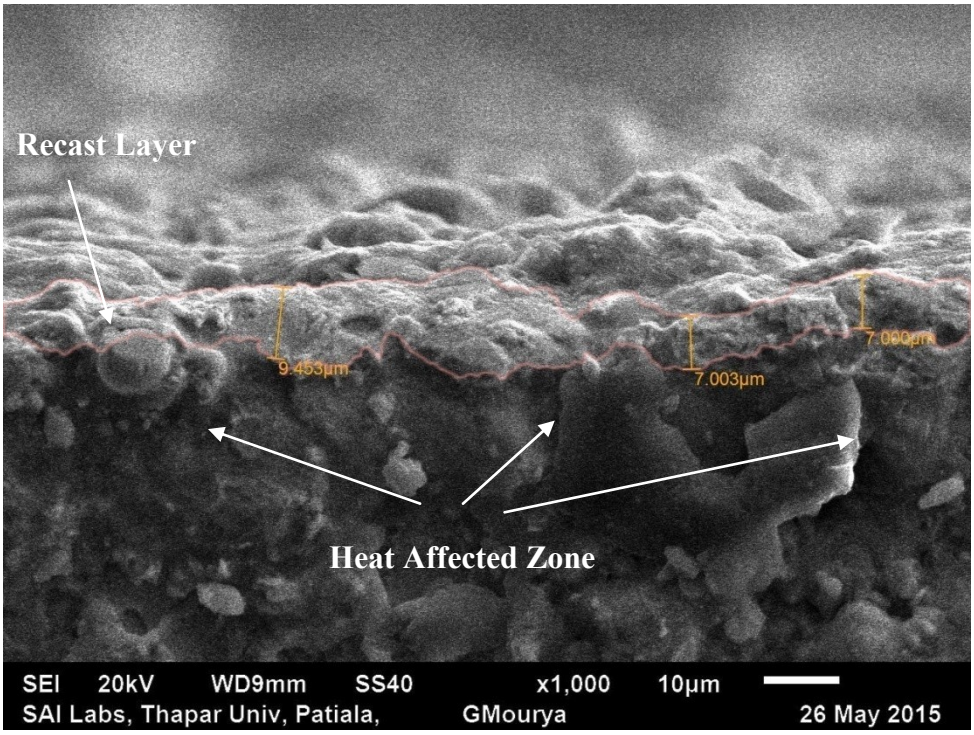

Figure 6.2: Recast Layer in sample machined with plain brass wire

Figure 6.3 shows the recast layer formed by zinc coated wire at parameters; T_{ON}=1.2 µs, T_{OFF}=26 µs, I_P=230 A and S_V=20 V. Both the specimen taken in this study are machined at same levels of parameters for better comparison for recast layer thickness. The mean thickness formed by zinc coated wire is 10.403 µm. It is observed on comparison that recast

layer thickness formed during machining with zinc coated wire is 20.33% more than that is formed by plain brass wire.

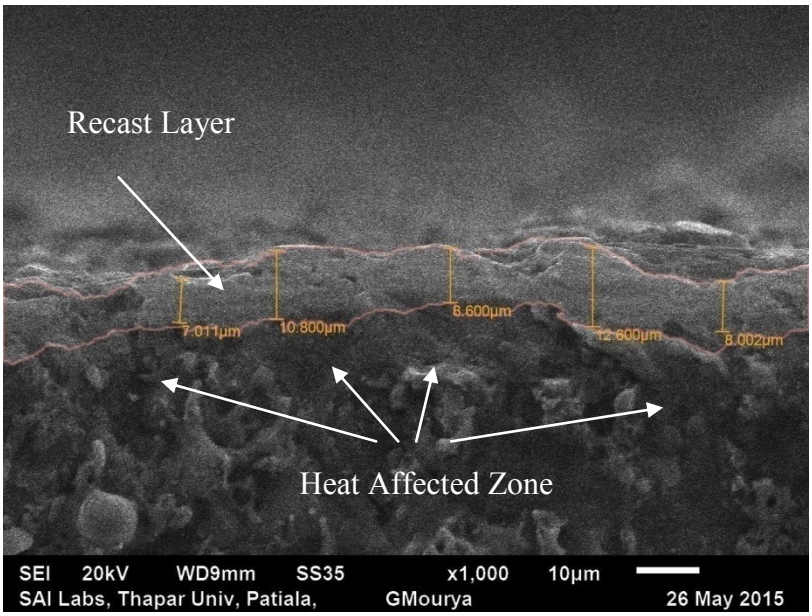

Figure 6.3: Recast Layer in sample machined with zinc coated brass wire

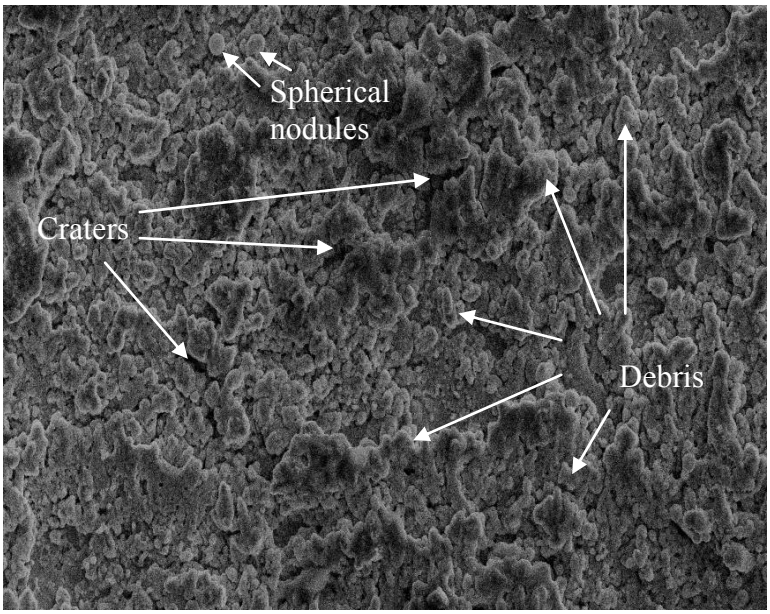

Figure 6.4: SEM image of surface machined with plain brass wire

The process parameters have an important role in the formation of machining surface. Generally, pulse on time, pulse off time, spark voltage and peak current are the main factors which influence the surface. The SEM images (Fig. 6.4 & Fig. 6.5) show the formation of globules of debris, craters, spherical nodules and cracks on the machined surface. Figure 6.4

shows the SEM micrograph taken from surface machined with plain brass wire and Fig. 6.5 shows the surface machined with zinc coated brass wire. As in Fig. 6.4, the amount of craters and debris is very high; this may be the reason for high surface roughness when machined with plain brass wire. Figure 6.5 shows lesser amount of globules of debris and deep or overlapping craters and hence a reason for less surface roughness.

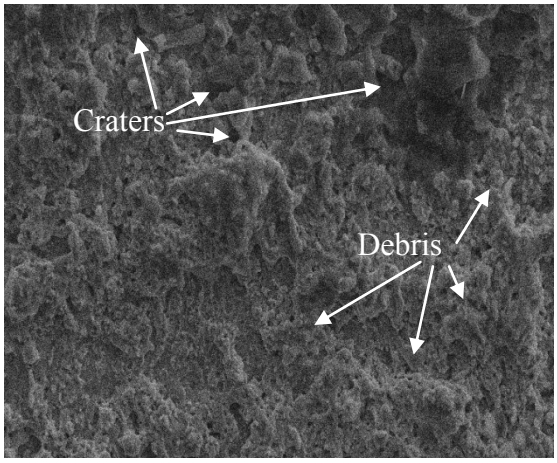

Figure 6.5: SEM image of surface machined with zinc coated brass wire

6.1.2 Energy Dispersive X-Ray Spectrometer (EDX)

The energy dispersive X-Ray spectrometer (EDX) is used to analyze the surface integrity of machined material. The EDX investigation reveals that the surface of sample machined with plain brass wire (Fig. 6.6) contains carbon, chromium, manganese, copper, zinc, calcium and oxides like $CaCo_3$, SiO_2. During discharge, the copper and zinc from the brass wire melts and re-solidifies on the workpiece surface in shape of debris or recast layer. As the machining is done in the presence of dielectric i.e. de-ionized water, the water droplets get decomposed due to discharge and vaporize easily and reacts with molten metal. The oxygen decomposed during discharge reacts with molten metal and form oxides on the metal surface. The EDX investigation for the sample machined by zinc coated brass wire (Fig. 6.7) reveals that the surface contains high amount of zinc, copper, calcium, chromium, manganese and oxides like $CaCO_3$, SiO_2, and FeS_2. The comparison between EDX results of both samples reveal that zinc concentration found in sample machined by coated wire more than found in sample machined by plain brass wire.

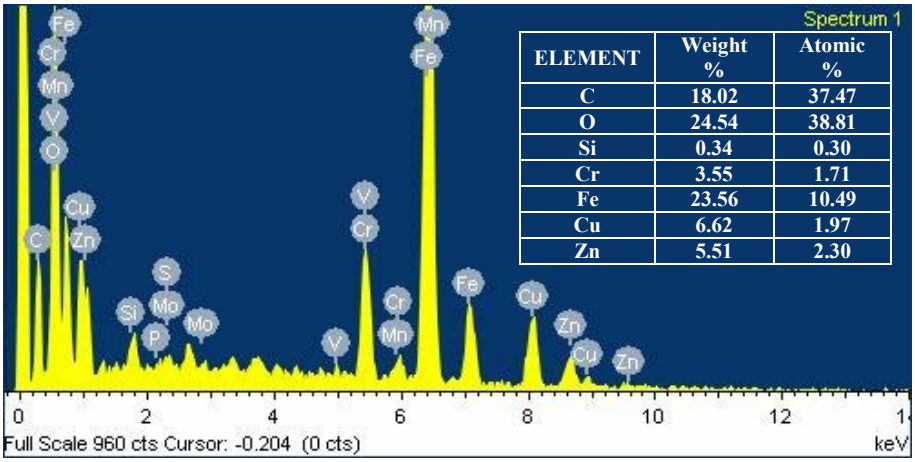

ELEMENT	Weight %	Atomic %
C	18.02	37.47
O	24.54	38.81
Si	0.34	0.30
Cr	3.55	1.71
Fe	23.56	10.49
Cu	6.62	1.97
Zn	5.51	2.30

Figure 6.6: EDX result for surface machined by plain brass wire

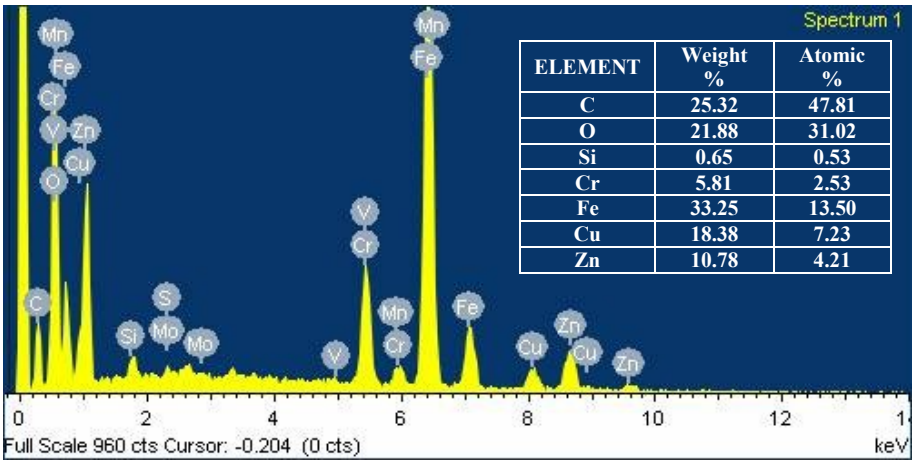

ELEMENT	Weight %	Atomic %
C	25.32	47.81
O	21.88	31.02
Si	0.65	0.53
Cr	5.81	2.53
Fe	33.25	13.50
Cu	18.38	7.23
Zn	10.78	4.21

Figure 6.7: EDX results for surface machined by zinc coated wire

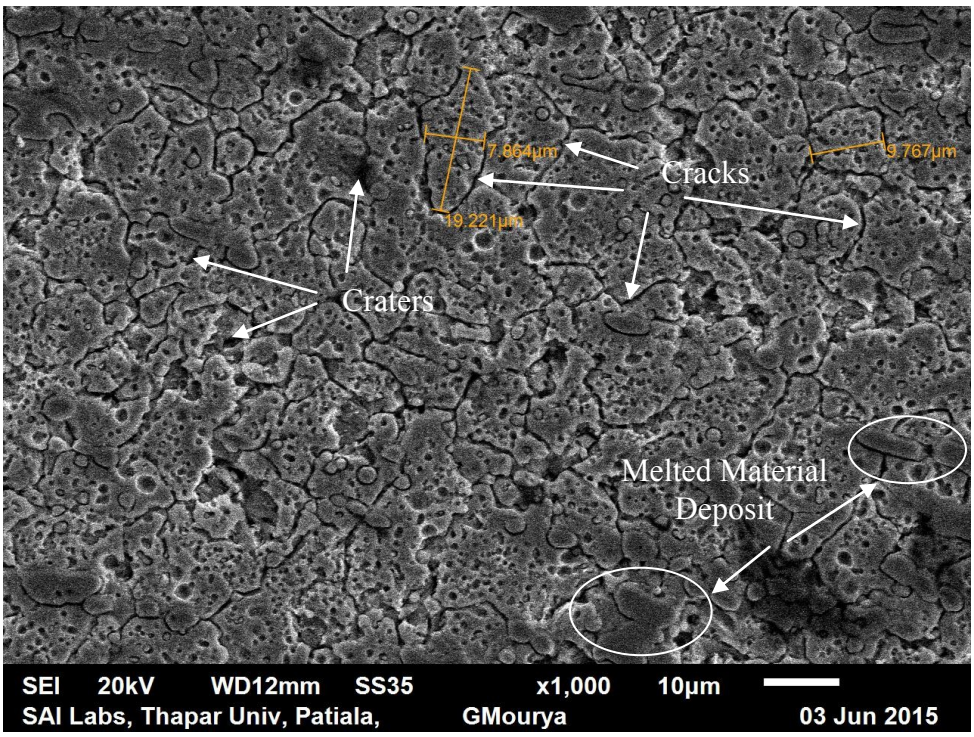

Figure 6.8: Surface machined with Plain Brass wire

The SEM micrograph in Fig. 6.8 & Fig. 6.9 show the surface obtained after removal of recast layer. The surface is polished and etching is done with Nital Acid which is suitable for D2 steel. The surface obtained is the heat affected zone (sub-surface) which contains micro-cracks, deep craters and melted material deposit. The discharge generally depend upon the peak current, pulse on time, pulse off time and servo voltage. As these samples are taken for high pulse on time, high peak current and low pulse off time as a result high thermal energy is induced in the workpiece surface and as dielectric is unable to sweep all the melted material during machining, tensile stress is generates in the surface. Generally cracks are formed when stress induced in the surface exceeds the ultimate tensile strength of the material. The comparison of both images reveals that the surface obtained by machined with brass wire (Fig. 6.8) has more number of craters, micro cracks and lesser melted material deposit than sample machined with zinc coated brass wire (Fig. 6.9).

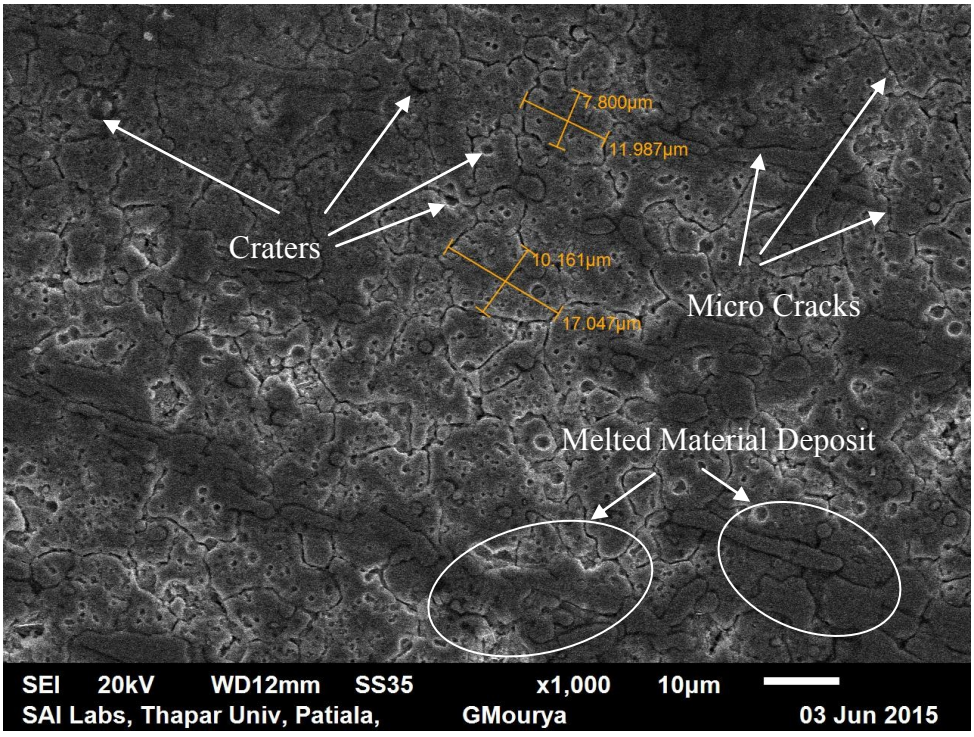

Figure 6.9: Surface machined with Zinc coated Brass wire

This chapter; although not conclusive, presents the preliminary investigation on the micro structural study and layer information deposited on the machined surface. This in turn, can be quite helpful for further investigation for generation of functionalized machined surface as well as an attempt towards minimization of subsurface damage of the work materials.

Chapter 7

Conclusions

7.1 Conclusions

In the earlier chapters, the details of preparatory research i.e. pilot study have been discussed to finalize the different process parameters and their working range for main experimentation. The main investigation is designed and executed using Taguchi's L18 orthogonal Array. The single response optimization is performed using Taguchi's delta statistics and multi response optimization is executed using Multi Response Signal Noise (MRSN) method. As the main experimentation is executed with two different wires viz., plain brass wire and zinc coated brass wire, so the results of performance characteristics are compared to determine better machining conditions for D2 steel

7.1.1 Pilot Study

Pilot investigation is performed with plain brass wire to identify significant parameters. The wide ranges of levels are varied for each process parameter to identify influence on cutting rate at each level. The pilot study is executed using one factor at a time (OFAT) approach which states only one factor can be varied at a time and other factors remain constant.

1) The pilot investigations revels that the pulse on time, pulse off time, peak current and spark gap set voltage have influenced the cutting rate (mm/min). The wire feed and wire tension failed to mark any significant effect on cutting rate and it remains almost constant on varying these two parameters.
2) Based on pilot experiments and literature review, the selected range or levels of WEDM process parameters are described in table 7.1.

Table: 7.1 Process parameters with levels

Factors	Parameters (Units)		Levels					
			1	2	3	4	5	6
A	I_P	Peak Current (A)	130	150	170	190	210	230
B	T_{ON}	Pulse on time (µs)	0.6	0.9	1.2	-	-	-
C	T_{OFF}	Pulse Off Time (µs)	19	26	34	-	-	-
D	S_V	Spark Gap Set Voltage (V)	20	30	40	-	-	-

7.1.2 Main Experimentation

The main investigation is executed with two different wires to their effect on machining characteristics which are material removal rate (mm^3/min), surface roughness (μm) and kerf width (mm). The main experimentation is performed using levels obtained from pilot study shown in table 7.1.

1) The findings from the experiments performed with plain brass wire are as follows:
   a. The results for MRR shows that it ranges from 2.81 mm^3/min to 9.97 mm^3/min. The percentage contribution of process parameters is as follows, pulse on time (72.77%), pulse off time (15.06%), peak current (8.53%) and servo voltage (1.59%).
   b. The results for individual increment in levels of parameters shows that when peak current was increased from 130 A to 230 A, MRR increase by 25.15%. When pulse on time was increased from 0.6 μs to 1.2 μs, the MRR increase by 63.63%. When pulse off time was increased from 19 μs to 36 μs, the MRR decreased by 34.79%. MRR decreased approximately by 11% when spark gap voltage was increased from 20 V to 40 V.
   c. The results obtained for surface roughness shows that it ranges from 1.63 μm to 3.49 μm. The percentage contribution of factors is as follows; pulse on time (70.53%), pulse off time (13.25%), peak current (3.16%) and spark gap set voltage (11.56%).
   d. The surface roughness was found to be increased by 44.19% when pulse on time is increased from 0.6 μs to 1.2 μs. The surface roughness decreased by 7.48% on increasing pulse off time from 19 μs to 36 μs. When spark gap voltage increased from 20V to 40V, the SR decreased by 13.61%
   e. The result for kerf width shows that it ranges from .259 mm to .329 mm. The percentage contribution of process parameters is as follows, pulse on time (53.24%), pulse off time (14.40%), peak current (29.70%) and servo voltage (0.72%).
   f. The results for individual increment in levels of parameters shows that when peak current was increased from 130 A to 230 A, kerf width increase by 11.07%. When pulse on time was increased from 0.6 μs to 1.2 μs, the kerf width increase by 14.15%. When pulse off time was increased from 19 μs to 36 μs, the kerf width

decreased by 6.90%. Kerf width decreased approximately by 1.41% when spark gap voltage was increased from 20 V to 40 V.

2) The findings from the experiments performed with zinc coated plain brass wire are as follows:
   a. The results for MRR show that it ranges from 3.63 mm^3/min to 12.09 mm^3/min. The percentage contribution of process parameters is as follows, pulse on time (70.53%), pulse off time (13.25%), peak current (3.16%) and servo voltage (11.56%).
   b. The results for individual increment in levels of parameters shows that when peak current was increased from 130 A to 230 A, MRR increase by 31.42%. When pulse on time was increased from 0.6 μs to 1.2 μs, the MRR increase by 49.17%. When pulse off time was increased from 19 μs to 36 μs, the MRR decreased by 25.95%. MRR decreased approximately by 15.52% when spark gap voltage was increased from 20 V to 40 V.
   c. The results obtained for surface roughness shows that it ranges from 1.85 μm to 3.10 μm. The percentage contribution of factors is as follows; pulse on time (82.76%), pulse off time (6.8%), peak current (2.73%) and spark gap set voltage (6.18%).
   d. The surface roughness was found to be increased by 36.80% when pulse on time is increased from 0.6 μs to 1.2 μs. The surface roughness decreased by 7.48% on increasing pulse off time from 19 μs to 36 μs. When spark gap voltage increased from 20V to 40V, the SR decreased by 8.04%
   e. The result for kerf width shows that it ranges from .269 mm to .343 mm. The percentage contribution of process parameters is as follows, pulse on time (53.26%), pulse off time (14.41%), peak current (29.71%) and servo voltage (0.72%).
   f. The results for individual increment in levels of parameters shows that when peak current was increased from 130 A to 230 A, kerf width increase by 11.61%. When pulse on time was increased from 0.6 μs to 1.2 μs, the kerf width increase by 15.01%. When pulse off time was increased from 19 μs to 36 μs, the kerf width decreased by 6.69%. Kerf width decreased approximately by 1.36% when spark gap voltage was increased from 20 V to 40 V.

3) The comparison of machining characteristics with both wires shows that
   a. MRR is increased by 24.98% with zinc coated brass wire as compared to plain wire.
   b. Surface roughness decrease by 7.54 % with brass wire compared to plain brass wire.
   c. The comparison shows an increase of 5.10% in kef width with coated wire.
4) The single response optimization is performed using Taguchi's delta statistics and optimal levels for parameters are selected.
   a. Table 7.2 shows the optimal levels of parameters for both wires.

Table 7.2 Optimal levels of parameters for both wires

Plain Brass Wire					
	Factor	I_P (A)	T_{ON} (µs)	T_{OFF} (µs)	S_V (V)
Material Removal Rate	Actual Value	230	1.2	19	20
	Optimum Level	6	3	1	1
Surface Roughness	Actual Value	190	0.6	34	40
	Optimum Level	4	1	3	3
Kerf Width	Actual Value	150	0..6	34	40
	Optimum Level	2	1	3	3
Zinc coated brass wire					
	Factor	I_P (A)	T_{ON} (µs)	T_{OFF} (µs)	S_V (V)
Material Removal Rate	Actual Value	230	1.2	19	40
	Optimum Level	6	3	1	3
Surface Roughness	Actual Value	190	0.6	34	40
	Optimum Level	4	1	3	3
Kerf Width	Actual Value	150	0.6	34	40
	Optimum Level	2	1	3	3

   b. The results obtained from confirmation experiments for single response optimization shows the improvement from the predicted results. Table 7.3 shows the results for confirmative experiments.

Table 7.3 Results of confirmative experiments for single response optimization

Plain Brass wire				
S. No.	Response	Predicted value	Experimental value	Change %
1	Material Removal Rate (mm^3/min)	10.99	11.41	3.82 %
2	Surface Roughness (µm)	1.69	1.33	21.30 %
3	Kerf Width (mm)	.261	.268	2.68
Zinc coated brass wire				
1	Material Removal Rate (mm^3/min)	12.99	14.30	10.14 %
2	Surface Roughness (µm)	1.85	1.50	18.9 %
3	Kerf Width (mm)	.245	.284	15.91 %

5) The multiple response optimization is performed using multi response signal noise (MRSN) method by applying equal weightage to surface roughness and material removal rate.

a. Table 7.4 shows the results for optimum levels.

Table 7.4: Optimum levels for MRSN

Plain Brass Wire				
Factor	I_P (A)	T_{ON} (µs)	T_{OFF} (µs)	S_V (V)
Actual Value	150	0.9	19	20
Optimum Level	2	2	1	1
Zinc coated brass wire				
Factor	I_P (A)	T_{ON} (µs)	T_{OFF} (µs)	S_V (V)
Actual Value	230	0.9	19	30
Optimum Level	6	2	1	2

b. The results for confirmative experiments are shown in table 7.5. The data show improvement in results.

Table 7.5: Error obtained for MRSN Plain brass wire

Plain Brass wire				
S. No.	Response	Predicted value	Experimental value	Error %
1	Material Removal Rate (mm^3/min)	-	6.97	-
2	Surface Roughness (µm)	-	2.40	-
3	MRSN (db)	-7.98	-7.86	1.50 %
Zinc coated brass wire				
S. No.	Response	Predicted value	Experimental value	Error %
1	Material Removal Rate (mm^3/min)	-	9.45	-
2	Surface Roughness (µm)	-	2.31	-
3	MRSN (db)	-8.07	-7.97	1.23 %

6) The SEM analysis of white layer thickness reveals that the average thickness obtained in plain brass wire is 7.184 µm and by zinc coated wire is 10.403 µm. The comparison shows that the layer thickness increased by 20.33% when coated wire is used to machine material.

7) The EDX analysis describes the addition of zinc, copper, calcium and oxides like $CaCO_3$, SiO_2 and other compound like FeS_2 were found on the machined surface of samples. The specimen machined with zinc coated wire shows high amount of zinc on the surface.

References

Abhinesh, P.; Varatharanjan, K.; Kumar, G.S. (2014) Optimization of process parameters influencing MRR, surface roughness and electrode wear during machining of titanium alloys by WEDM. *International Journal of Engineering Research and General Science,* 2(4): pp. 719-729.

Antar, M.T.; Soo, S.L.; Aspinwall, D.K.; Jones, D.; Perez, R. (2011) Productivity and workpiece integrity when WEDM aerospace alloys using coated wires. *1st CIRP Conference on Surface Integrity,* 19: pp. 3-8.

Bhatia, A.; Kumar, S.; Kumar, P. (2014) A study to achieve minimum surface roughness in Wire EDM. *International Conference on Advances in Manufacturing and Materials Engineering,* 5: pp. 2560-2566

Chabra, S.; Gupta, D.; Yadav, P. (2014) Optimizing the process parameters of WEDM using Taguchi technique on P-21 die steel. *International Journal of Innovative Research in Science ,Engineering and Technology,* 3(7); pp. 14815-14821.

Dhobe, M.M.; Chopde, I.K.; Gogte, C.L. (2013) Effect of heat treatment and process parameters on surface roughness in WEDM. *International Journal of Mechanical Engineering and Robotics Research*, 2(2): pp. 275-281.

Dhobe, M.M.; Chopde, I.K.; Gogte, C.L. (2014) Modeling and optimization of WEDM parameters for surface finish using design of experiments. *Proceedings of the 2014 International Conference on Industrial Engineering and Operations Management,* pp. 1830-1839.

Gaitonde, V.N.; Karnik, S.R.; Achyautha, B.T.; Siddeswarappa, B. (2006) Multi-response optimization in drilling using Taguchi's quality loss function. *Indian Journal of Engineering & Material Science*, 13: pp. 484-488.

Goyat, L.; Dudi, R.; Sharma, N. (2013) Investigation of process parameters contribution and their modeling in WEDM for D-2 tool steel using ANOVA. *Global Journal of Engineering, Design and Technology,* 2(3): pp. 41-46.

Hascalyk, A.; Caydas, U. (2004) Experimental study of wire electrical discharge machining of of AISI D5 tool steel. *Journal of materials Processing Technology,* 148: pp. 362-367.

Huang, J.T.; Liao, Y.S. (2003) Optimization of machining parameters of WEDM based Grey relational and statistical analyses. *International Journal of Production Research*, 41(8): pp. 1707-1720.

Ikram, A.; Mufti, N.A.; Saleem, M.Q.; Khan, A.R. (2013) Parametric Optimization for Surface Roughness, kerf and MRR in WEDM using Taguchi design of experiment. *Journal of Mechanical Science and Technology,* 23(7): pp. 2133-2141.

Jangra, K.; Jain, A.; Grover, S. (2010) Optimization of multiple machining characteristics in wire electrical discharge machining of punching die using Grey Relational analysis. *Journal of Scientific and Industrial Research,* 69: pp. 606-612.

Kern, R. (2007) EDM Wire Primer. *EDM Today,* (7): pp. 10-17.

Khundrakpam, N.S.; Singh, J.; Singh, K.; Kumar, S. (2014) Effects of WEDM process parameters on surface roughness. *International Journal of Mechanical Engineering and Robotic Research,* 3(2): pp. 435-441.

Kumar, A.; Kumar, V.; Kumar, J. (2012) Prediction of surface roughness in WEDM process based on response surface methodology. *International Journal of Engineering and Technology,* 2(4): pp. 708-719.

Kumar, V.M.; Babu, A.S.; Ventatasamy, R.; Raajenthiren, M. (2010) Optimization of the WEDM parameters on Machining Incoloy800 super alloy with multiple quality characteristics. *International Journal of Engineering Science and Technology,* 2(6): pp. 1538-1547.

Lee, L.; Lim, L.; Wong, Y. (1992) Towards crack minimisation of EDMed surfaces. *Journal of Materials Processing Technology*, 32(1): pp. 45–54.

Maan, V.; Chaudhary, A.; (2013) Optimization of WEDM of D-2 Steel using Response Surface Methodology. *International Journal of Engineering Research and Application,* 3(3): pp. 206-216.

Mahapatra, S.S.; Patnaik, A. (2006a) Parametric Optimization of WEDM process using Taguchi method. *Journal of the Brazilian Society of Mechanical Science and Engineering*, 27(4): pp. 422-429.

Mahapatra, S.S.; Patnaik, A. (2006b) Optimization of WEDM process parameters using genetic algorithm. *Indian Journal of Engineering & Material Science*, 13: pp. 494-502.

Mahapatra, S.S.; Patnaik, A. (2007) Optimization of WEDM process parameters using Taguchi method. *International Journal of Advanced Manufacturing Technology*, 34: pp. 911-925.

Patil, P.A.; Wahgmare, C.A. (2014) Optimization of process parameters in WEDM using response Surface Methodology. *Proceedings of 10th IRF International Conference,* pp. 110-115.

Ramakrishnan, R.; Karunamoorthy, L.; (2006) Multi response optimization of wire EDM operations using robust design of experiments. *International Journal of Advance Manufacturing Technology*, 29: pp. 105-112.

Ramasawmy, H.; Blunt, L.; Rajurkar, K. (2005) Investigation of the relationship between the white layer thickness and 3D surface texture parameters in the die sinking EDM process. *Precision Engineering,* 29(4): pp. 479–490.

Shah, A.; Mufti, N.A.; Rakwal, D.; Bamberg, E. (2011) Material Removal Rate, Kerf and Surface Roughness of Tungsten Carbide Machined with WEDM. *Journal of Material Engineering and Performance*, 20(1): pp. 70-76.

Sharma, N.; Khanna, R.; Gupta, R. (2013) Multi quality characteristics of WEDM process parameters with RSM. *International Conference on Design and Manufacturing,* 64: pp. 710-719.

Shivdev, A.S.; Shinde, V.D. (2014) Multi-objective optimization in WEDM of D3 tool steel using integrated approach on Taguchi method and Grey relational analysis. *Journal of Industrial Engineering International*, 10(4): pp.149-162.

Singh, H.; Garg, R. (2009) Effects of process parameters on material removal rate in WEDM. *Journal of Achievements in Materials and Manufacturing Engineering,* 32(1): pp. 70-74

Singh, H.; Khanna, R. (2011) Parametric Optimization of Cryogenic-Treated D-3 for Cutting Rate in Wire Electrical Discharge Machining. *Journal of Engineering and Technology,* 1(2): pp. 59-64.

Singh, N.; Kumar, P.; Goyal, K. (2013) Effect of two different cryogenic treated wires in wire electrical discharge machining of AISI D3 die steel. *Journal of Mechanical Engineering,* 43(2), pp. 54-60.

Sommer, C.; Sommer S. (2005) Complete EDM Handbook. Advance Publishing Inc, Texas.

Sudharsun, D.; Durairaj, M.; Swamyanathan, N. (2013) Analysis of process parameters in Wire EDM with Stainless Steel using Single Objective Taguchi method and Multi objective grey relational grade. *International Conference on Design and Manufacturing,* 64, pp. 868-877.

Tai, T.; Lu, S. (2009) Improving the fatigue life of electro-discharge-machined SDK11 tool steel via the suppression of surface cracks. *International Journal of Fatigue,* 31(3): pp. 433–438.

Tilekar, S.; Das, S.S.; Patowari, P.K. (2014) Process parameters optimization of WEDM on Aluminum and Mild Steel by using Taguchi Method. *International Conference of Advances in Manufacturing and Materials Engineering,* 5: pp. 2577-2584.

Tosun, N.; Cogun, C.; Tosun, G. (2004) A study on kerf and material removal rate in wire electrical discharge machining based on Taguchi method. *Journal of Materials Processing Technology,* 152: pp. 316-322.

Vates, U.K.; Singh, N.K.; Singh, R.V. (2014) Modeling of Process Parameters on D2 steel using Wire Electrical Discharge Machining with combined approach of RSM and ANN. *International Journal of Scientific & Engineering Research,* 5(1): pp. 2026-2035.

Web References

W.1 What is Wire EDM ?, www.jacksmachine.com/pdf/what-is-wire-edm.pdf, (accessed on – 14/12/2014)

W.2 D2 Tool Steel, http://www.azom.com/article.aspx?ArticleID=6214, (accessed on – 12/06/2015)

List of Publications

1. Amanpreet Singh and Hiralal Bhowmick (2015) "Optimization of WEDM process parameters on D2 steel for different wire materials", *Proceedings of the Institution of Mechanical Engineers, Part B: Journal of Engineering Manufacture.*

   .....Communicated

2. Amanpreet Singh and Hiralal Bhowmick (2015) "Influence of the process variables on the MRR of AISI D2 steel in WEDM", *International Journal of Multi Disciplinary Engineering and Business Management*. 3(3): pp 74-78

   .....Published